White Covers
also Title Page

NASA CR-66709

DESIGN AND CONSTRUCTION OF AN EXPANDABLE AIRLOCK

By Kenneth R. Berg, Ph.D.

Prepared under Contract No. NAS 1-5752 by
Whittaker Corporation/Research and Development Division/San Diego

for

NATIONAL AERONAUTICS AND SPACE ADMINISTRATION

TABLE OF CONTENTS

Blank page

DESIGN AND CONSTRUCTION OF AN EXPANDABLE AIRLOCK

Prepared by Kenneth R. Berg
Whittaker Corporation, Research & Development Division/San Diego

ABSTRACT

An expandable airlock structure was designed, built, and tested by Whittaker Corporation, Research & Development Division/San Diego as an engineering model to be used by NASA-Langley engineers to determine the feasibility of an isotensoid structure for an airlock function. The design utilized the latest in flexible structural fabric materials and an isotensoid design for maximum structural efficiency. High efficiency glass reinforced epoxy was used in the hatch door and skirt. The design operating pressure is 15 psig with an ultimate burst pressure design strength of 50 psig. The airlock was proof pressure tested to 29.4 psig without damage. A retraction mechanism allows minimum volume storage when not in use.

INTRODUCTION

The success of our manned space probes is partly contingent upon the development of efficient space vehicle apparatus that will inflict minimal weight and volume penalties against the total payload. One such apparatus is an airlock, a pressure vessel which will permit the transference of men and materiel between regions of differing pressure, either within or external to the space vehicle proper. Since actual use of an airlock will be intermittent, the concept of a lightweight, expandable structure has emerged as the most efficient design approach to this particular problem. For transfer operations external to the space vehicle, an expandable airlock deployed externally would provide additional volume and would allow the airlock to be designed for internal pressure loads only. For internal operations, an expandable airlock could be stored in a minimum of volume and erected only when needed.

Under a previous NASA contract*, Whittaker Research & Development/San Diego explored the feasibility of designing an expandable airlock based on the elastic recovery principle, whereby the stored potential energy of a compressed material is used as the deployment mechanism. Once feasibility had been demonstrated, detailed design and construction of a prototype model was necessary in order to complete the evaluation of this approach. Essentially, an airlock assembly had to be fabricated to meet the requirements for easy crew transfer, micrometeoroid protection, thermal protection, maximum flexibility, multiple deployment-retraction cycles, and minimum leakage.

Under the present program, a prototype airlock assembly was designed, fabricated, and tested structurally by Whittaker, assisted by Astro Research Corporation, the major subcontractor for this program. This is a report on the findings of that program.

---

* Contract NAS 7-283, "Research on an Expandable Airlock Utilizing the Elastic Recovery Principle," monitored by Mr. J. Williams, Langley Research Center. Reference NASA CR-351, dated November 1965.

55 % Top on Page 3

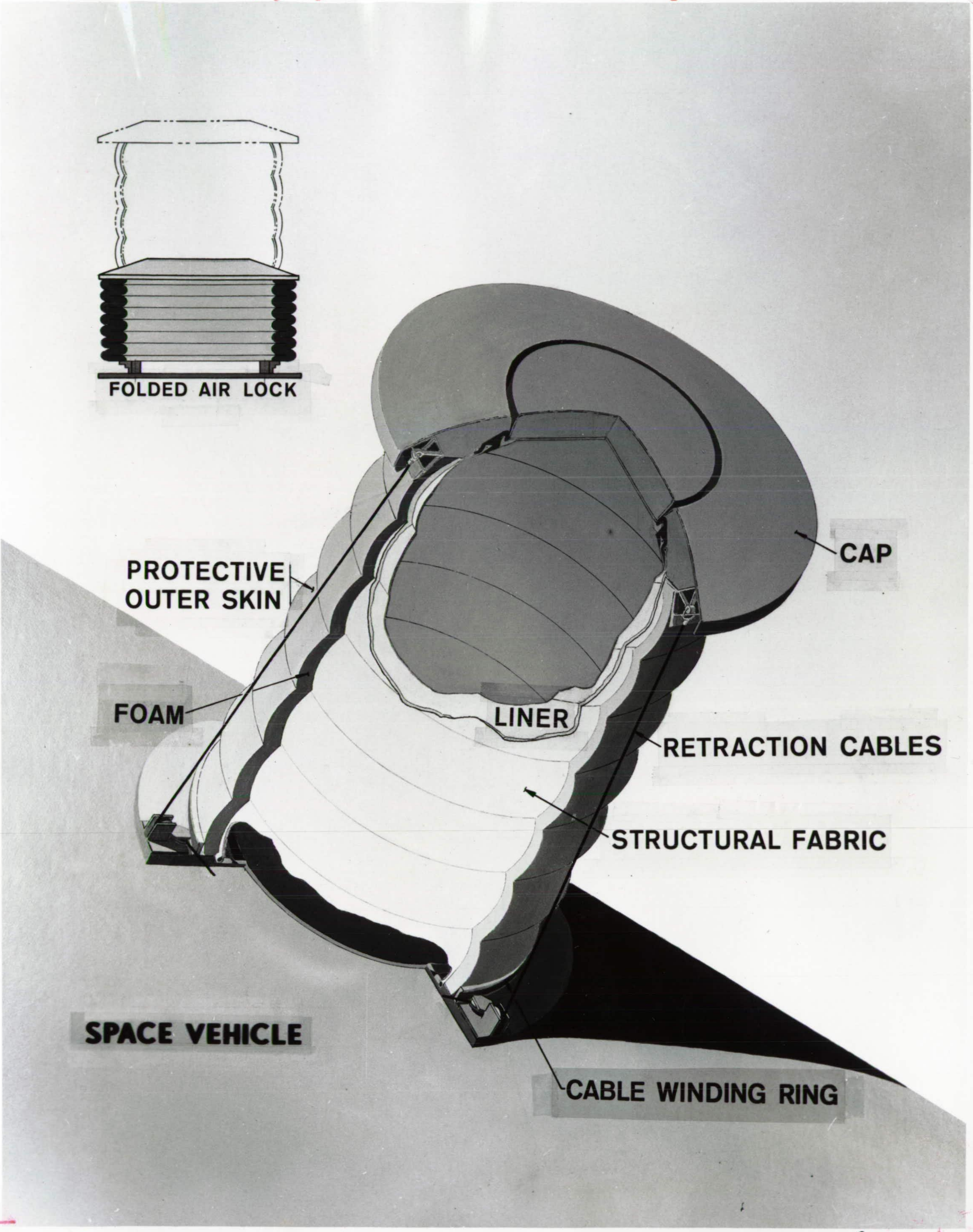

DESIGN APPROACH AND GOVERNING CRITERIA

The expandable airlock concept is depicted in Figure 1. As designed, the expandable airlock is 4 feet in diameter and 7 feet in length in its equilibrium condition, with an axial expanded-to-retracted volume ratio of 7-to-1. In its retracted state, the airlock length is about 20 inches, the length being limited by limit switches. The basic principle controlling the design and construction is that of elastic recovery, whereby the stored potential energy of the foamed plastic walls will, in the folded configuration, act to deploy the airlock to its fully extended condition.

The principle parts of the airlock are the flexible folding cylinder, the hatch, the baseplate, and the retraction mechanism. The retraction mechanism includes the retraction cables, the retraction ring upon which the cables are wound, and the electric motor, gear reducer, sprockets, and roller chain for turning the ring.

Figure 1 depicts the airlock in both the expanded and retracted position.

Figure 1. Design Concept of the Expandable Airlock

Figure 2 shows the configuration of the convoluted foam cylinder; Figure 3 depicts the composition of the cylinder wall. The convolutions are created by hoops of glass filament-wound epoxy rings. The ends of the cylinder are closed by end plates, to which the end rings are clamped. The pressure liner is a tailored, film fabric composite bag. The entire structure is covered with a multilayer micrometeoroid bumper of two layers of flexible foam, and three layers of tightly knitted Dacron cloth. Figure 4 shows the structural fabric, comprised of load-carrying fibers and the knitted Dacron monofilament.

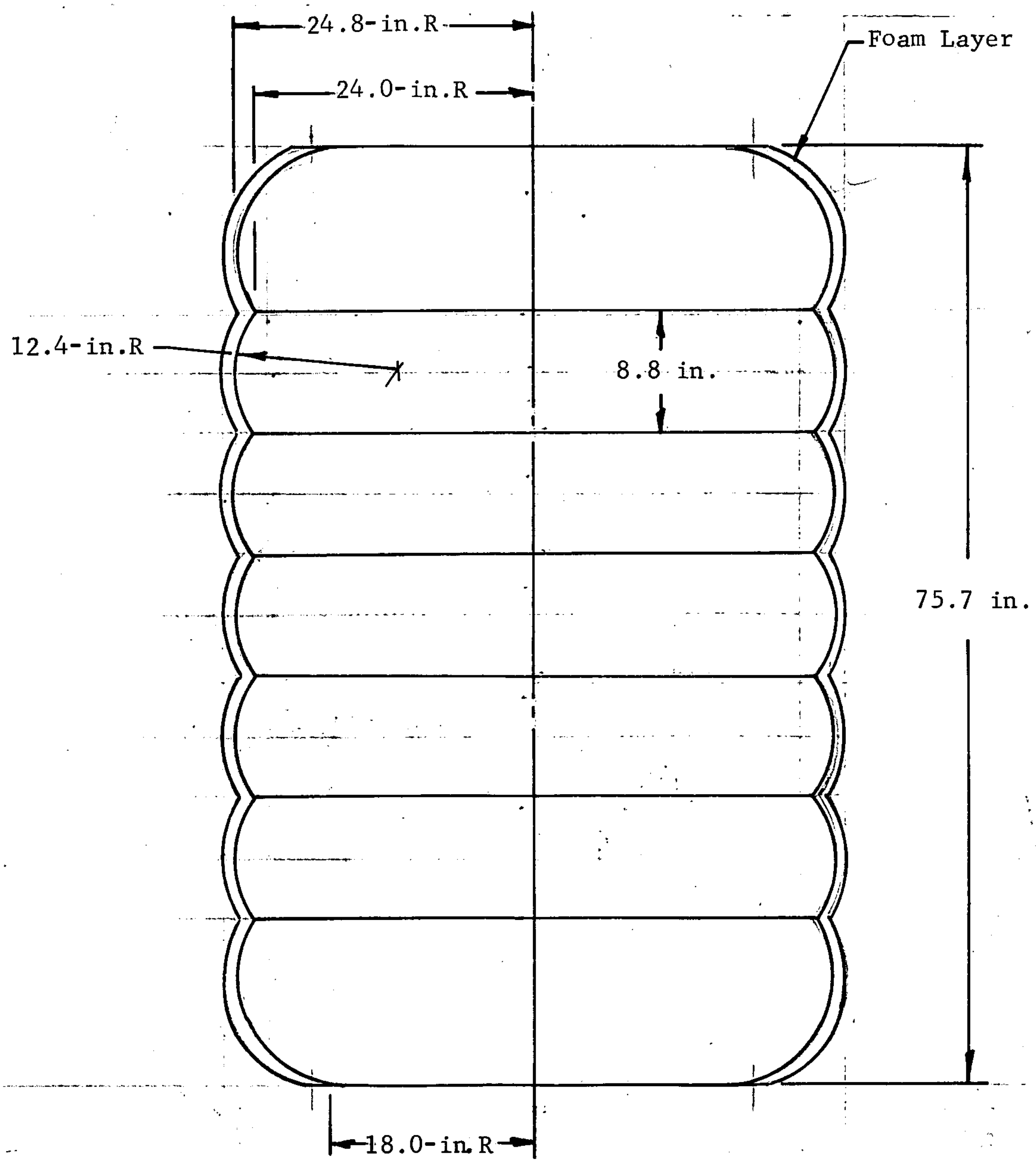

Figure 2. Convoluted Foam Cylinder

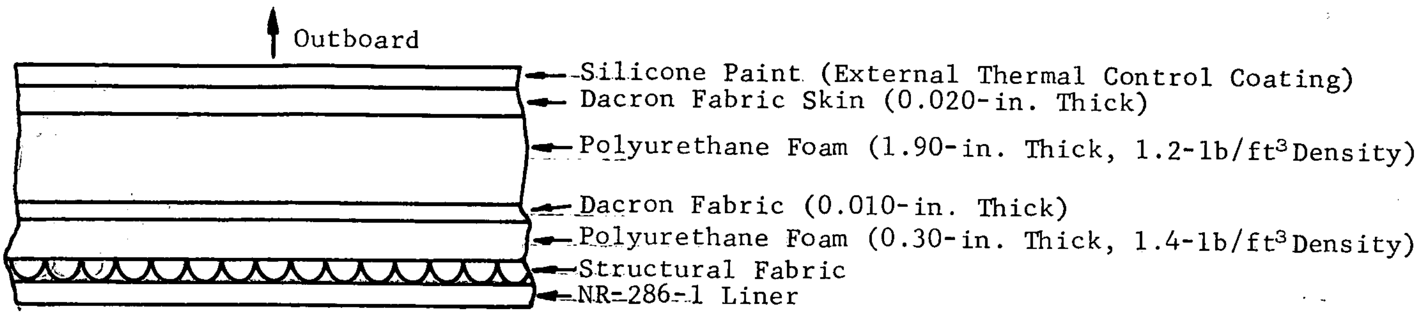

Figure 3. Constituents of Airlock Wall

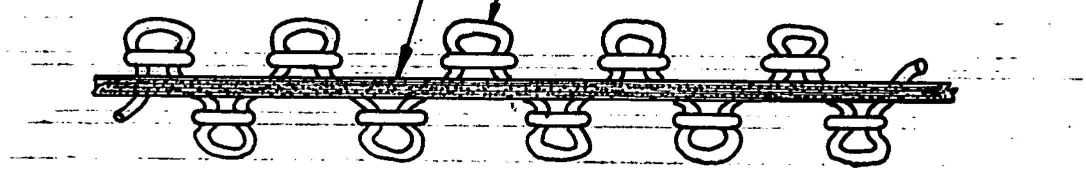

(a) Top View

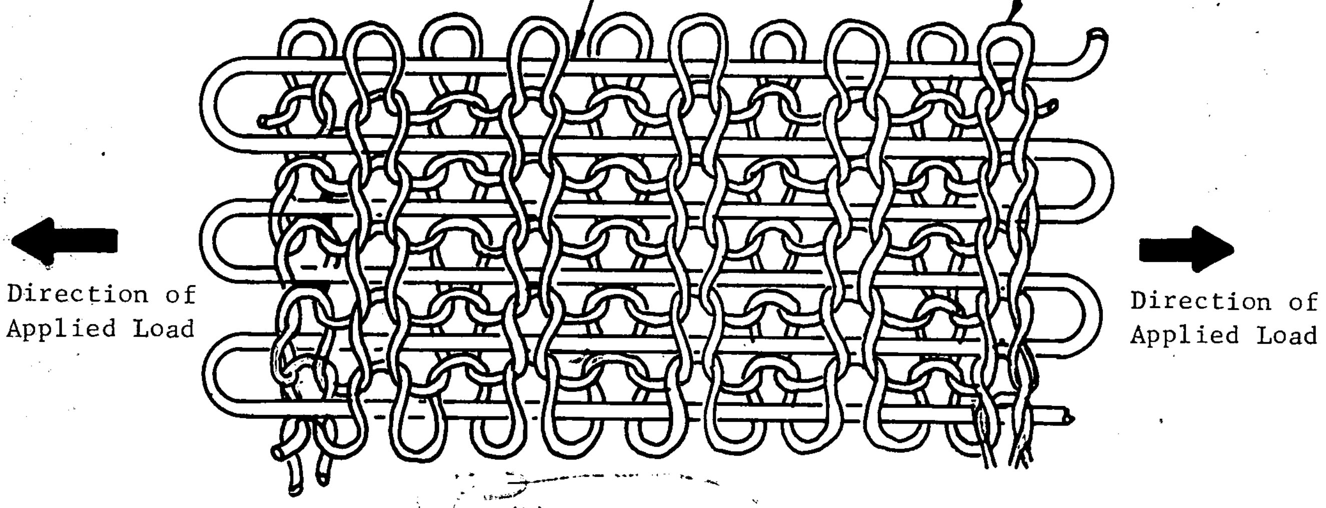

(b) Side View

Figure 4. Views of Structural Fabric, Showing the Load-Carrying Fibers Held in Place by Knitted Dacron Monofilament

The airlock is deployed from its collapsed configuration by easing the pull on the retracting cables, using the stored energy of the compressed foam to extend the chamber to its maximum length. To retract the airlock, an electric motor drives a roller chain, rotating a sprocket that winds the retracting cables onto the retracting ring. The retracting cables are attached to a ring assembly at the outer (upper) end of the airlock assembly. The lock is maintained in the retracted condition by means of continued tension of the retracting cables. The retraction mechanism is depicted schematically in Figure 5.

The overall design concept emerged in response to the following criteria:

1. The expanded airlock dimensions must be sufficient to allow one man in a pressurized space suit to perform the operations (opening hatches, closing valves, etc.) necessary for ingress and egress.

2. The structure must be designed for minimum weight and for maximum expanded-to-packaged volume ratio.

3. The internal surface of the airlock and hatch passageways must be free from all surface discontinuities which might damage a space suit.

4. Construction materials must be nontoxic and suitable for use in a hard vacuum (10^{-6} Torr) with a minimum of outgassing, and must also be compatible with argon, nitrogen, helium, freon, and oxygen (to be used as test media during subsequent pressure testing).

5. The airlock and associated equipment must be designed to withstand a positive pressure of 1 atmosphere pressure differential, with a safety factor of 3.4 based on the failure strength of the materials.

6. The hatch door must be equipped with a quick-closure device, compatible with the design concept, which can be operated from either side by one man with a maximum handle force of 25 pounds.

7. The hatch door must be equipped with a valve having zero leakage, and sized to permit the pressure defferential across the door to be balanced within 60 seconds. The valve must be capable of being controlled manually from either side of the hatch door. The hatch door must also be equipped with pressure gages to indicate the pressure differential when viewed from either side of the door.

8. The airlock must be designed for minimum leakage.

9. The hatch seals must be designed and housed to offer maximum protection from operational use, yet must provide easy access for repair or replacement.

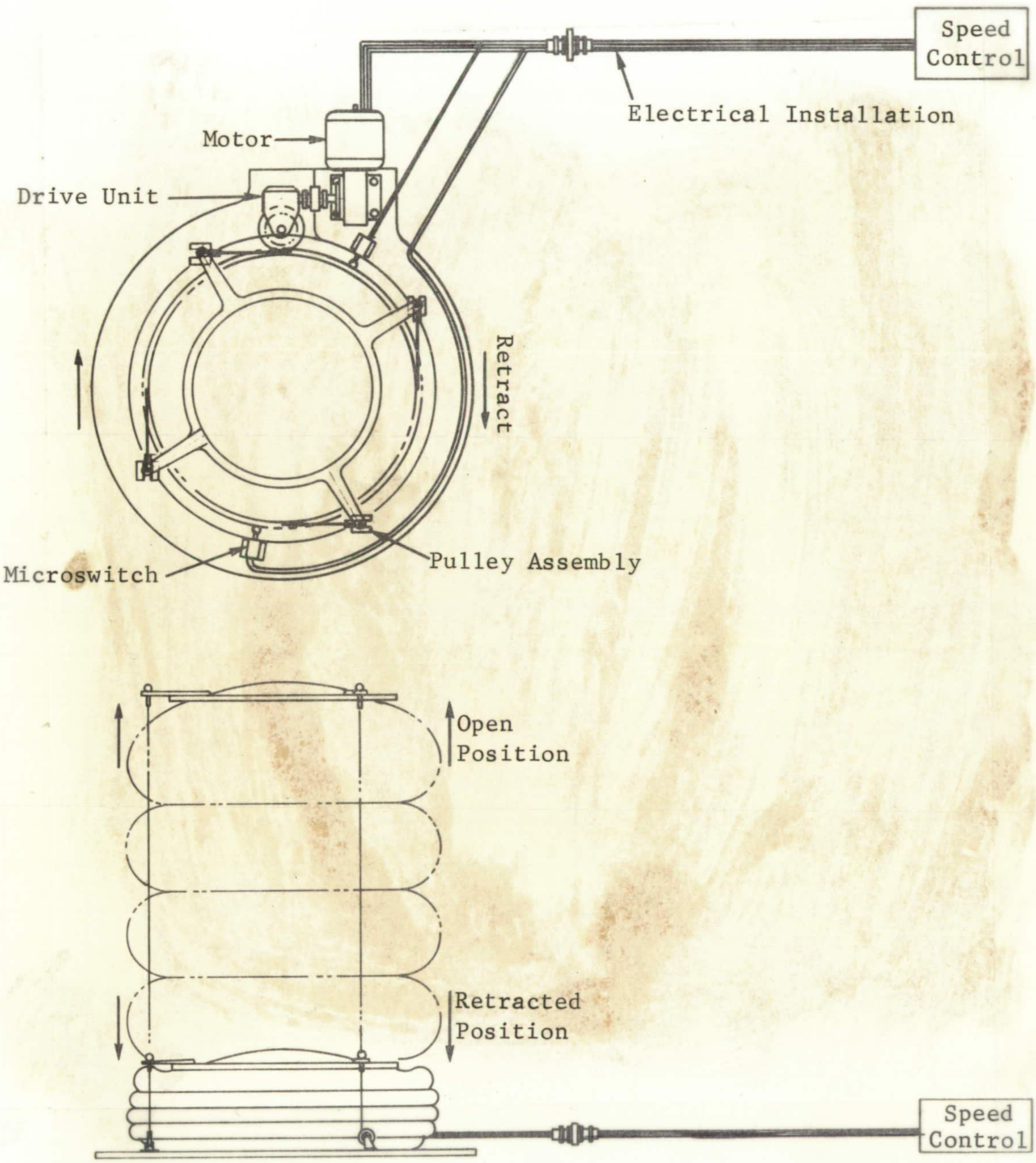

Figure 5. Retraction Mechanism

Additional parameters against which the prototype airlock would be tested included the following:

1. Since the airlock assembly or components will be required to operate in a vacuum environment for as long as 1 year, leak rates must be measured for 30 to 60 days during initial testing.
2. During its service life, the airlock structure and associated equipment (excluding seals) must be capable of withstanding 1000 pressure loading cycles under static and ambient temperature conditions without degradation of its sealing effectiveness.
3. The airlock assembly must meet requirements for an operating pressure of 1.0 atmosphere (14.7 psig), a proof pressure of 2.0 atmospheres (29.4 psig), and a burst pressure of 3.4 atmospheres (50.0 psig).

The detailed test plan which was used to guide testing of the expandable airlock is included as Appendix A to this report.

DESIGN ANALYSIS

The detailed calculations for the loads and stress analysis conducted for the airlock components appear in Appendixes B through I. The weight analysis is included as Appendix J. Complete design drawings, upon which these calculations were based, have been presented separately. Table I is a summation of the margins of safety for the airlock components and Table II presents the weight tabulations, both estimated and actual.

TABLE I

SUMMATION OF FACTORS OF SAFETY

Component	Margin of Safety
Base Plate Cover (NR-285)	+21.00
Top End Ring (NR-291)	--
Dome — Inverted Dome Junction:	
Aluminum Ring (NR-295)	+0.40
Dome	+0.83
Inverted Dome w = 0°	+2.03
w = 5°	+0.92
w = 10°	+1.02
Hatch (NR-296):	
Press Load	+1.43
Dome Edge Discontinuity	+0.11
Hatch Ring (NR-295)	+1.98
Baseplate (NR-284):	
Baseplate	+1.34
Bolt Holes	+0.31
Top Ring (NR 291):	
Stress	+2.38
Outer Segment	+20.48
Bolt Holes	--

TABLE II

EXPANDABLE AIRLOCK STRUCTURAL WEIGHT TABULATION

Part Identification	Dwg No.	Est Wt, Lb	Actual Wt, Lb
Retraction Ring Assembly	NR-287	14.72	16.5
Drive Unit	NR-289	42.00	44.5
Top Ring Assembly	NR-291	31.2	36.0
Structural Fabric Retainers	NR-292	19.9	19.0
Hatch Ring	(NR-295)	(3.15)	--[5]
Hatch Dome	(NR-296)	(3.74)	--[3]
Bleed Valve Installation	(NR-299)	(3.27)	--[3]
Adhesive	--	(0.25)	--[3]
Hatch Assembly	NR-294	10.41[1]	10.5[2]
Hatch Latch Assembly	NR-297	0.31	--[3]
Idler Pulley Assembly	NR-298	0.97	1.2
Cable Tensioner	NR-300	0.47	--[5]
Roller Spacer	NR-301	0.58	3.5[4]
Seals	NR-302	1.49	--[5]
Cable Attach Arm	NR-303	1.8	--[5]
End Rings	NR-352	2.02	2.02[6]
Liner (with end O-rings)	NR-286-1	11.9	9.5
Elastic Recovery	--	38.0	36.55
Bolts, Cables, etc.	--	36.0	18.0
Structural Fabric (with hoops)	ARC 1985	16.0	18.0
Total Structural Airlock Weight:		227.8	213.3

[1] Total of hatch ring, hatch dome, bleed valve installation, and adhesive.

[2] Total of same items as [1], plus hatch latch assembly.

[3] Included in [2].

[4] Includes cable tensioner, seals, and cable attach arm.

[5] Included in [4].

[6] Included in structural fabric.

NOTE: Total weight before shipping was actually 488.75 pounds, including base plate and base plate cover. Total weight of airlock less fixture and drive mechanism was 152.3 pounds.

R

AIRLOCK FABRICATION

Basically, the component fabrication sequence was divided into three areas: fabrication, component subassembly, and final assembly. Actual fabrication and assembly of the airlock took place at Whittaker Corporation, Research & Development Division/San Diego. The structural fabric was supplied by Astro Research Corporation[1], and the large end rings and base plate were procured from Circlemaster of El Cajon, California. Standard quality control measures were observed throughout each stage of fabrication. Design drawing numbers and their LRC counterparts are listed in Appendix J.

Airlock Component Fabrication

Hatch Assembly. The configuration of this part is presented in Drawing NR-294. The following fabrication method was used to prepare this component.

Before layup commenced, the plaster male and female contour surfaces were given two coats of paste wax and one coat of polyvinyl chloride (PVC) film release, each coat being allowed to dry before the next was applied.

Eight 38- x 38-inch plies were cut from 181 Style E-glass fabric with a Volan A finish. The required 1500 style bleeder material and PVA bag material were also cut, and assembled for use near the work area. The bag sealing tape was then adhered to the tooling, with the paper backing intact. The aluminum stiffener ring was degreased with methyl ethyl ketone (MEK) and masked on all surfaces except the laminate bonding area. The bonding area was chemically cleaned with an H_2SO_4-$Na_2Cr_2O_7$-H_2O etchant solution. This procedure was followed by an MEK rinse and air-dry. Reference Figure 6.

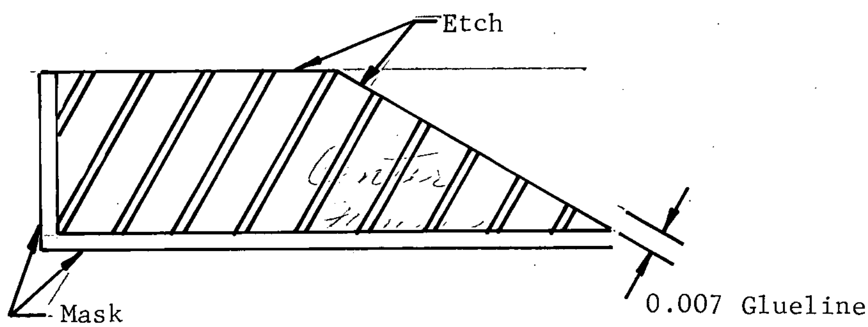

Figure 6. Hatch Layup
Figure 6

Using clean polyethylene gloves, the fabrication technician then centered the aluminum ring, using shims, into the tool recess (see Figure 7).

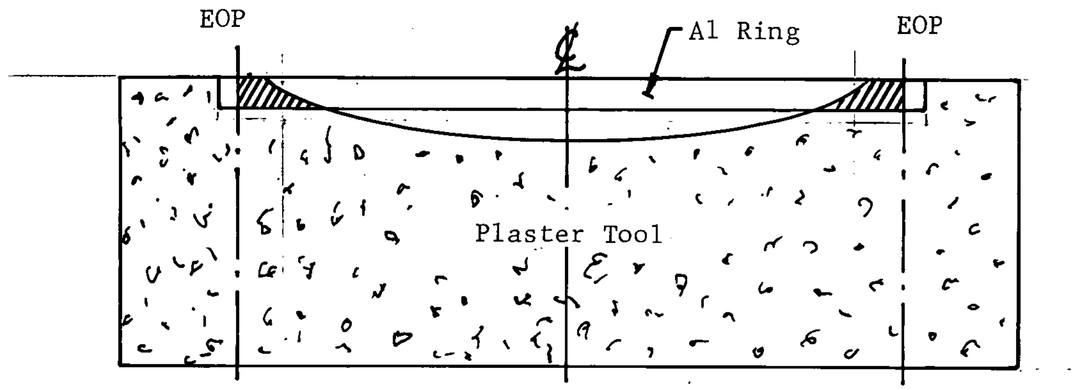

Figure 7. Laminate Tool Contour

A resin system comprised of 1000-grams of Epon 815 resin and 80 grams of Furane 951 plastics hardener was uniformly applied to the plaster tool and the aluminum ring bonding surfaces (see Figures 7 and 8).

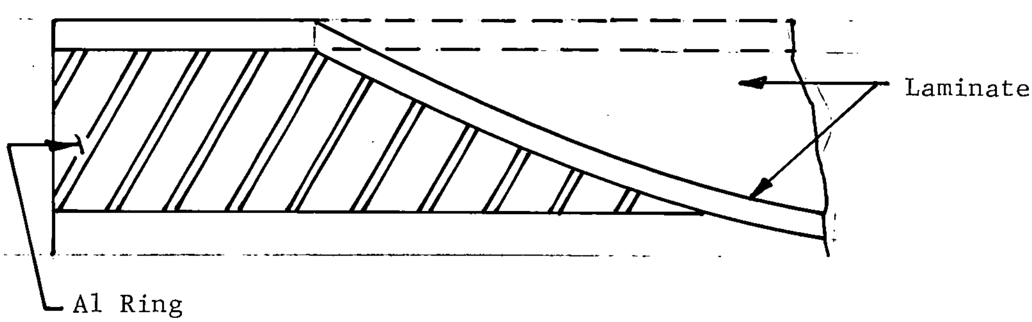

Figure 8. Detail of End-of-Part

The 181 glass fabric plies were then laid up on the tool and aluminum ring bonding surfaces, each ply being impregnated thoroughly and uniformly. Figure 9 shows the warp orientation used.

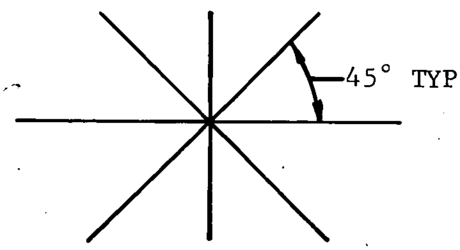

Figure 9. Warp Orientation

Here, two 5-inch diameter plies were cut and laid up, one between the third and fourth plies, and the other between the fifth and sixth plies, concentric to 4.25-inch diameter, flat at the centerline.

The paper from the sealing tape previously adhered to the tool and bag part was then removed. The part was placed under 28 in. Hg pressure, and all excess resin and air entrapments were squeegeed to the bleeder at the edge of the part. The part was then cured overnight at room temperature, under 28 in. Hg vacuum pressure.

The following day, the bag material was removed and the edge of the part was trimmed on a turntable. The part was then postcured for 1 hour at 200° ±10°F while still on the plaster tool, followed by a 2-hour cool-down period.

Once the part had cooled sufficiently, a hole was cut, per Design Drawing NR-296, and the part was removed from the tool. The entire laminate surface was sanded in order to achieve a smooth surface finish. Following a rinse with MEK and an air-dry, the laminate surface was given a final thinned resin coat (100-phr Epon 815 resin, 12-phr Furane 951 plastics hardener, and 10-phr MEK) and allowed to cure at room temperature in a dust-free atmosphere.

After the final cure, the maskout was stripped from the aluminum ring, which was wiped with MEK and air-dried. The laminate adjacent to the ring was masked off, and the ring was etched, rinsed as before, then given a final water rinse, an MEK rinse, and an air-dry. The cleaned, dried aluminum surface was finally brush-alodized and dried, and the part was ready for assembly.

Figure 10 shows the fiberglass hatch dome being assembled.

#5540

#5838

Figure 10. Assembly of Fiberglass Hatch Dome

Structural Fabric. The configuration of this fabric was shown previously in Figure 4 (page 5). The fabric originally was comprised of Type 51 Dacron fiber, cabled and heat-stretched, and Type 0-7 nylon monofilament. However, later testing showed another material was required in order to improve the reliability of the load-carrying strings. The newer material was Type 73 Dacron yarn, six strands (each 1100 denier) twisted into a single cable (6600 denier). The 51 strands were cabled into a 2 by 3 cable with two strands twisted together (5.3 turns per inch), and the three sets of two-strand cables twisted together (2.5 turns per inch). The cables were hot-stretched to reduce subsequent elongation, and were not given a coating application.

The following fabrication procedure was used. The Dacron string was wound on a 25.41-inch diameter drum, as shown in Figure 11, and markings were applied at circumferential intervals of 0, 18.5, 26.88, 33.61, 43.34, 53.07, 61.80, and 79.95 inches. Markings were also made on both sides of these markings, at a 1-inch distance. The string was then respooled from the drum onto the bobbin for further processing on the knitting machine.

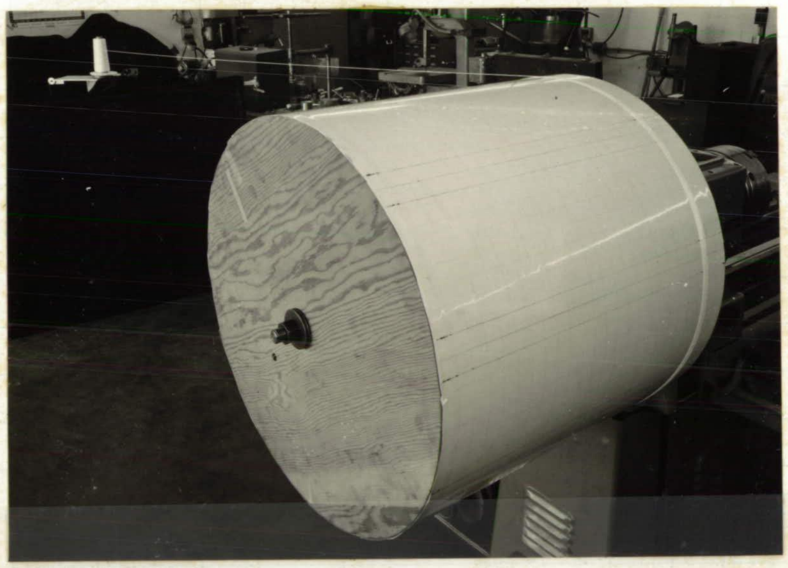

Figure 11. Longitudinal Fiber Marking Drums

1248

Six fiberglass hoop rings comprised of B-stage epoxy-coated and 20-end S-HTS S-717 roving, were then fabricated by winding preimpregnated S-glass tape onto the split mandrel shown in Figure 12.

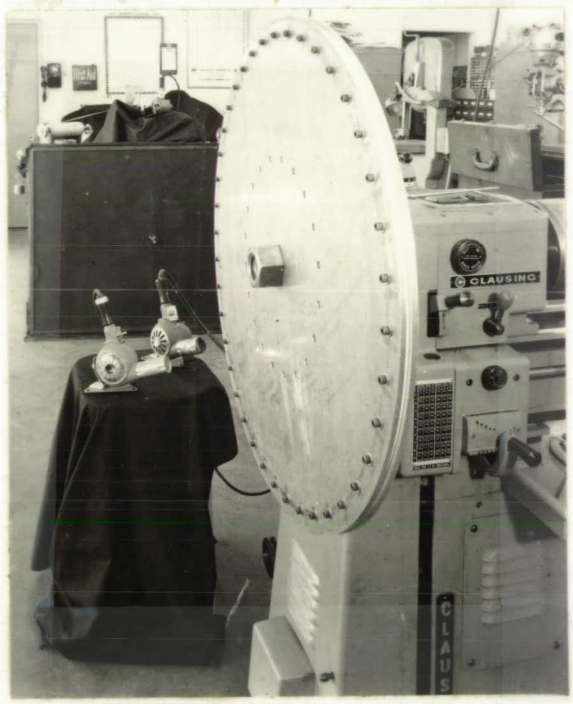

Figure 12. Winding Apparatus

The knitting machine was prepared by inserting rings into roller tracks, as shown in Figure 13. The structural filaments were included at this point in the operation. Figure 14 illustrates the resulting structural fabric. It might be pointed out here that, as originally planned, the load-carrying fiber was embedded in every second row of knitted Dacron monofilament. Subsequent difficulties, described later in this report, led to a design where the load-carrying fiber was embedded in every row of Dacron monofilament, as depicted earlier in Figure 4.

Figure 13. Astroflex Knitting Machine with End Rings Installed

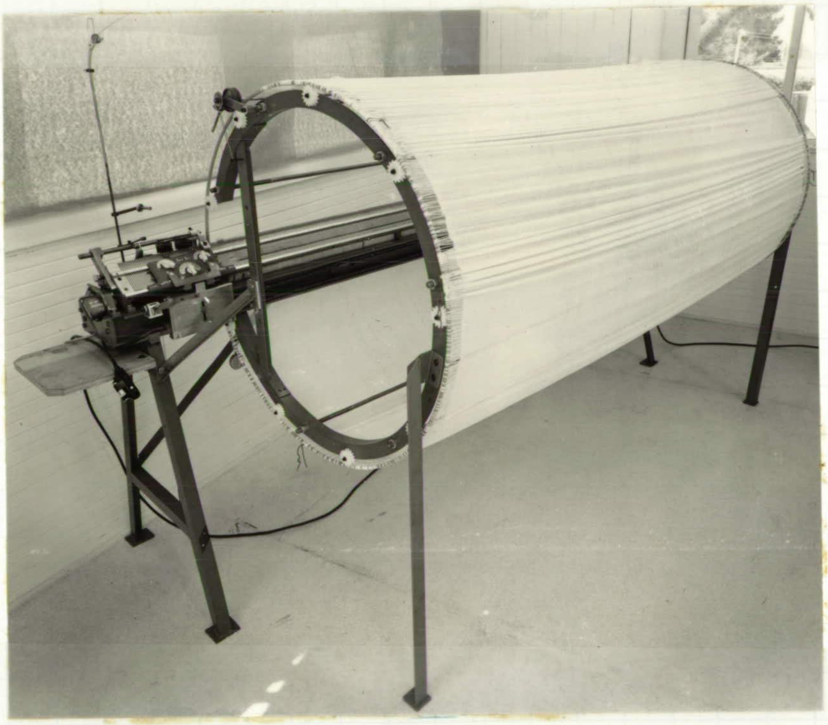

Figure 14. Knitted Fabric Ready for Sewing

Once the fabric was produced, the beginning and end stitches were woven together, making 1 knit and 1 purl stitch. The knitted fabric was attached to the hoop rings by a basting stitch, as shown in Figure 15. The fabric was then removed from the knitting machine and placed on a support stand, where the hoops were slipped over the fabric and expansion rings were inserted to span the fabric between hoops.

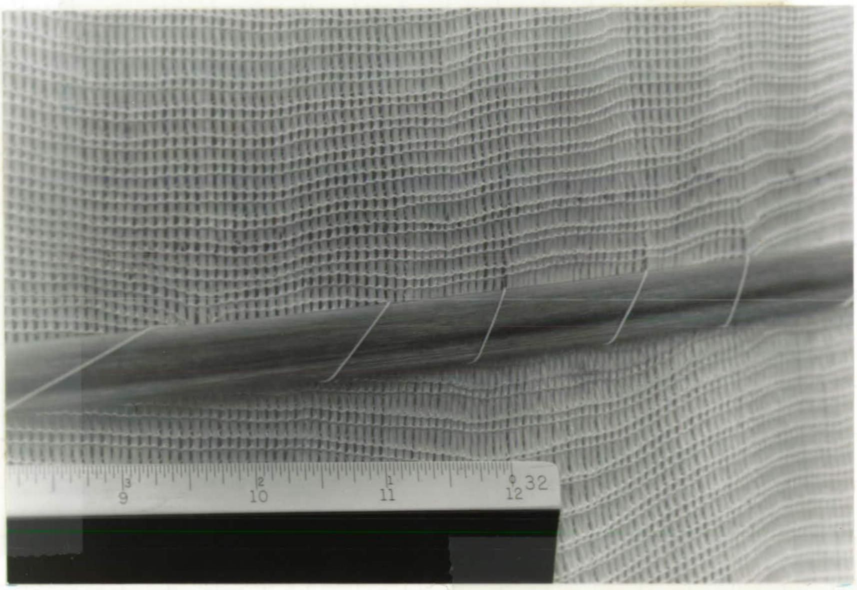

Figure 15. Method used to Position Hoop Rings onto the Structural Fabric

The epoxy-glass hoops were then bonded to the knitted structure by the following method.

The hoops were prepared with an acetone wash, a light sand faying of the surface, and another acetone wash to remove dust. They were given a final acetone wipe, and a dry wipe, immediately before being stored in a dry, dust-free area prior to bonding.

The adhesive was prepared by weighing 100-pbw Adiprene L-100 into a flask and heating it to 212°F, followed by a degassing in a vacuum jar and a cooldown period to 150°F. MOCA (12.5 pbw) was then dissolved in acetone (100 pbw) and the mixture was added to the Adiprene.

As the first step in the actual bonding procedure, the hoops were located between the expansion rings per design dimensions. With the liner in place, a slight pressure (0.5 psi) was applied to the airlock. The position of the hoops was again checked, and the location then marked accurately on the fabric. The pressure was then removed and the liner taken out. The alignment was checked, as well as the hoop location. The adiprene adhesive was applied from the inside of the structure, using a 1/2-inch wide brush to avoid runoff. The lower one-third of each hoop was bonded first, with the entire assembly being turned until the entire hoop region was coated. The assembly was then allowed to cure overnight at room temperature. The following day, a second coat of Adiprene adhesive (made with 80-pbw rather than 100-pbw acetone) was applied. The assembly was cured at room temperature for 3 days.

Figure 16 shows the hoops after bonding to the structural fabric. Figure 17 shows the completed airlock fabric structure.

(a) Inner View

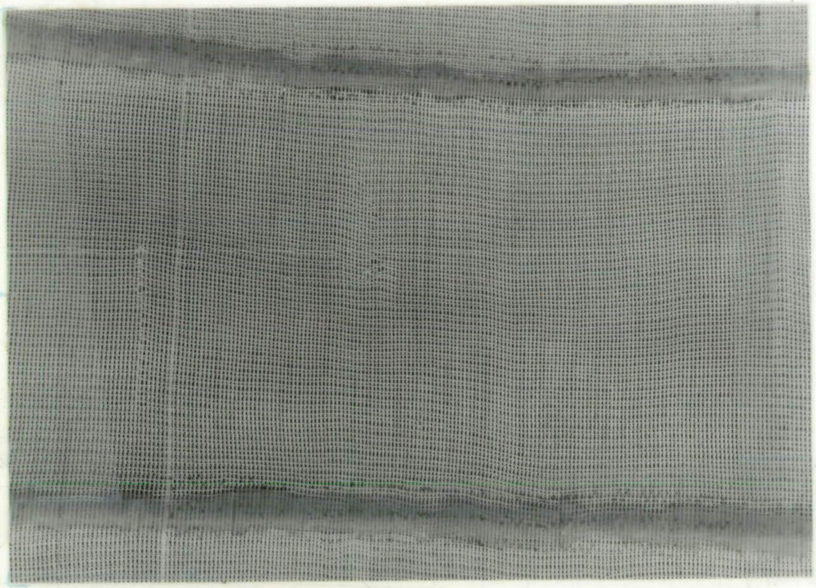

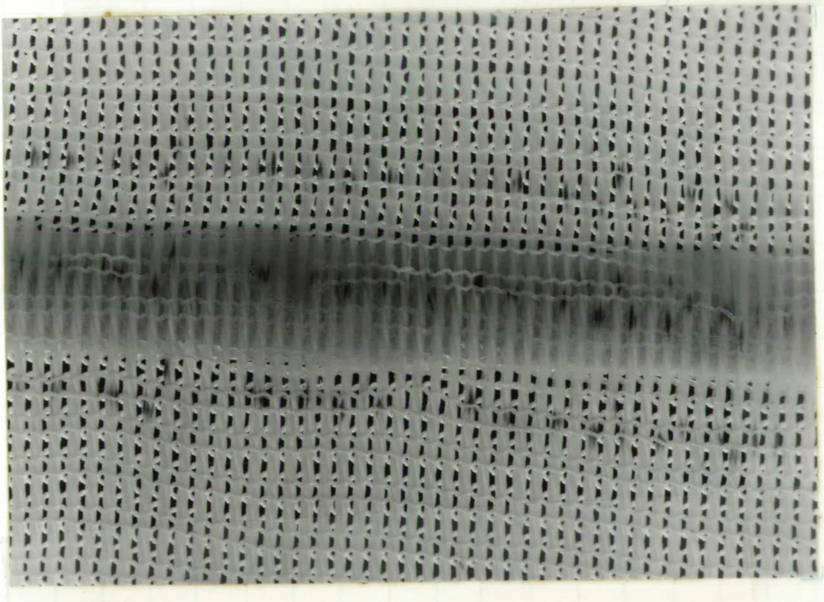

(b) Outer View

Figure 16. View of Hoop Bands after Bonding to Structural Fabric

Figure 17. Completed Airlock Fabric Structure on Support Stand

TOP

On pg 90

Structural Assembly for Proof Testing

Before the final prototype airlock could be assembled, a pressure test had to be conducted on a structural test assembly, comprised of the structural fabric, the liner, the base closure plate and seals, the end ring retainers, the hatch end ring and seal, and the hatch assembly. See Figure 18.

Figure 18. Airlock Structural Test Assembly

The unit was to be disassembled following successful completion of the test. However, the structural fabric failed to pass the required proof pressure test and a second structural test assembly had to be built, this time with the improved configuration mentioned in the preceding section.

Airlock Body Fabrication and Final Assembly

The final steps in the fabrication phase of the program involved reassembling the liner inside the pressure-tested structural fabric, assembling the rest of the component parts in place, then applying the elastic recovery and protective materials to the structural fabric.

Figures 19 through 22 depict the airlock in various stages of assembly. Figure 23 shows the pressurized (1.5 psi) airlock ready for the application of the outside layers.

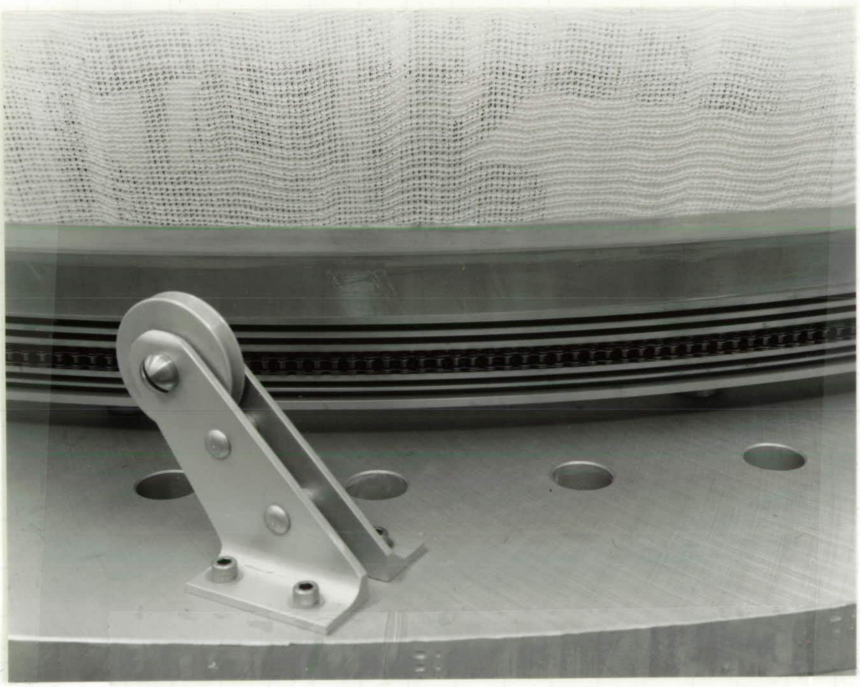

ENLARGE

Figure 19. Retraction Roller Chain and Cable Pulley

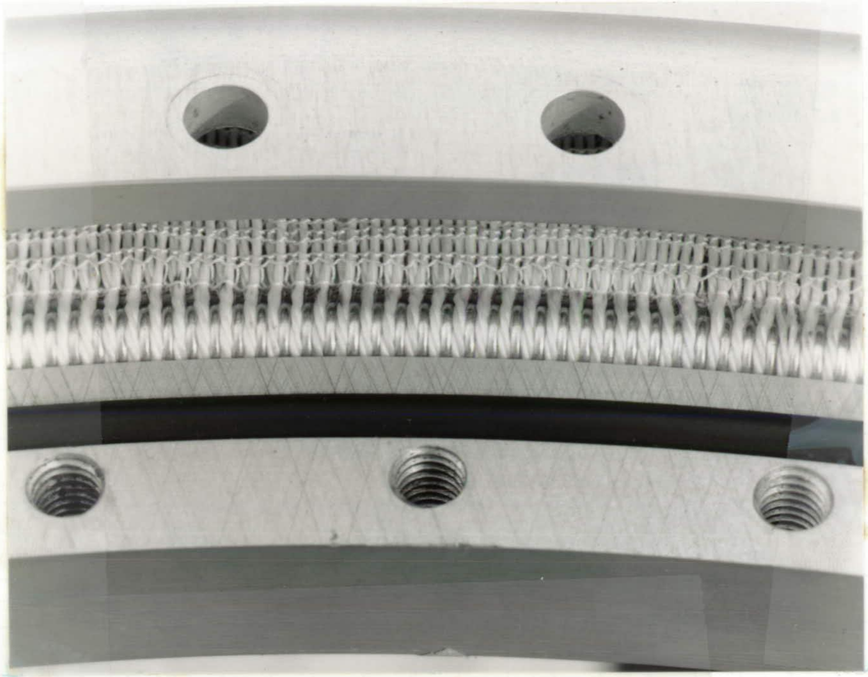

Figure 20. Hatch Seal and Grooved End Ring; Structural Fabric in Place

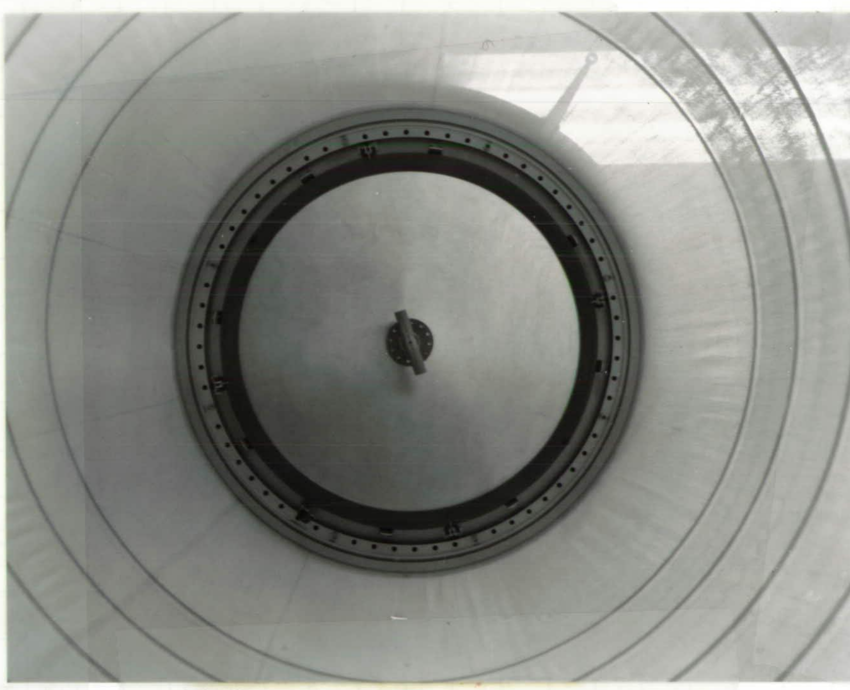

Figure 21. Completed Hatch Dome and Handle in Place

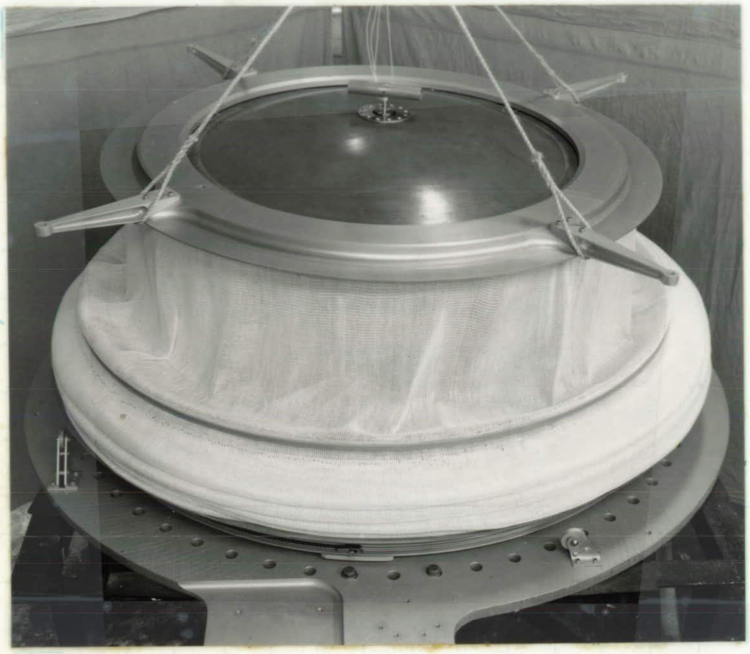

Figure 22. Structural Fabric and Hatch Assembled

Figure 23. Pressurized Structure Ready for Installation of Micrometeoroid Foam and Dacron Fabric

The following procedure was used in bonding the foam layers to the airlock assembly.

Enough Adiprene and MOCA (about 800 grams) to cover eight 12- x 80-inch sheets of release paper was weighed out. The MOCA was then melted and mixed with Adiprene (preheated to 150°F). Eight sheets of release paper were coated with a 0.007-mil thick film of the Adiprene-MOCA mixture, and left to stand for 2 hours. (For the sake of convenience, two sheets were prepared at a time, using a 200-gram batch of the resin coating.)

Two 78- x 43-inch swatches of Dacron cloth were then cut at the ends, then laid down on a Mylar-covered work table. The resin-coated release paper was laid on the cloth, one layer at a time, with each layer overlapping the other about 1 inch. The release paper was stripped off before the following layer was applied.

Next, 0.30-inch thick foam sheet was laid out on a plywood caul covered with Kraft paper. The impregnated Dacron cloth was stripped from the tabletop and laid on the foam. Once wrinkles had been smoothed out, the layup was covered with release paper and weighted with another section of plywood. The layup was cured for 12 hours at room temperature.

From the Dacron-foam sandwich sheets, four 10- x 80-inch strips were cut from each sheet. A pattern was then made by following two fabric twines, 10 inches apart, on the inflated airlock. A 3/8- x 4-inch cut was made on both sides of each 10-inch swatch to accommodate the radius differential caused by the fiberglass rings (see Figure 24).

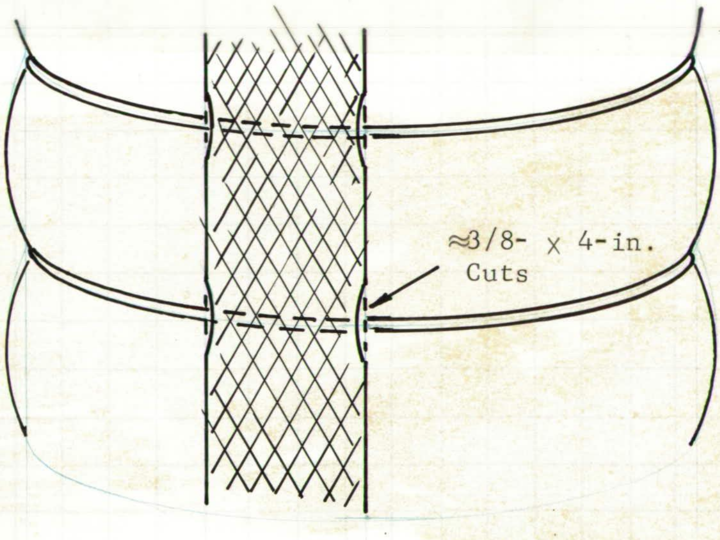

Figure 24. Adjusting Dacron-Foam Strips to Airlock Contour

All 16 gores were then taped in place, with necessary alterations being made at that time. The tape was left on for 12 hours in order to preform the Dacron-foam gores. Each gore was then numbered as to its prefit location and removed from the airlock. A transfer coat of 0.007-mil Adiprene-MOCA was applied to the foam side of each gore and to one side edge. The gores were then relocated and held snugly in place with masking tape over each splice. One-inch wide cellophane shrink-tape was wound over the ring areas. Thin nylon film and 1500 glass cloth were used to apply pressure over the wide areas. All necessary repairs were made prior to bonding the 1.90-inch foam.

The 1.90-inch foam horizontal panels were prefit, starting at the lower glass-wound ring, and then taped in place and located. For the area near the hatch, three full pieces were split in order to fill the area between the first prefit circle and the shield net. The same coating and layup operations described before were accomplished, except in this case the concave side, one edge, and one end of each piece were coated, and then allowed to stand 2-3 hours to produce the desired tack. The pressure blankets were removed after the cure, and small imperfections were repaired.

TESTING

The plan for testing the expandable airlock is delineated in Appendix A. This plan was followed closely, except that the leakage test was deleted by mutual agreement between NASA-LRC and Whittaker.

In brief, the load-carrying fabric failed during the first proof pressure test. After analysis was made of the failure and its possible causes, appropriate tests were conducted in order to pinpoint the proper corrective action. Using the results from these tests as guidelines, a second fabric/liner section of the airlock was fabricated. This revised section was tested successfully to full proof pressure. Tests of the retraction mechanism also yielded satisfactory results.

First Proof Pressure Test

The structural fabric and liner was pressure-tested on 28 December 1966 at Whittaker Corporation, Research & Development Division/San Diego. It was to be proof tested to 2 atmospheres (29.4 psig) but failed catastrophically at 27.7 psig. Failure occurred in the structural fabric at the top end ring, causing the following damage:

1. The structural fabric was destroyed.
2. The liner was destroyed.
3. The top end ring was slightly warped but still usable.
4. The bond between the hatch ring and the laminate was partially delaminated.
5. Two seals were damaged.

The test sequence and some of the resulting damage are shown in Figures 25 through 29. Figure 25 shows the airlock at the start of testing and after partial pressurization. Figure 25 illustrates the instrumentation used for a rough measurement of circumferential expansion. Figures 27 and 28 are progressively more detailed views of the damage suffered by the structural fabric, concluding with the failed ends of the load-carrying strings or cords. Figure 29 shows the delamination of the hatch dome.

L

#67-24 #67-22

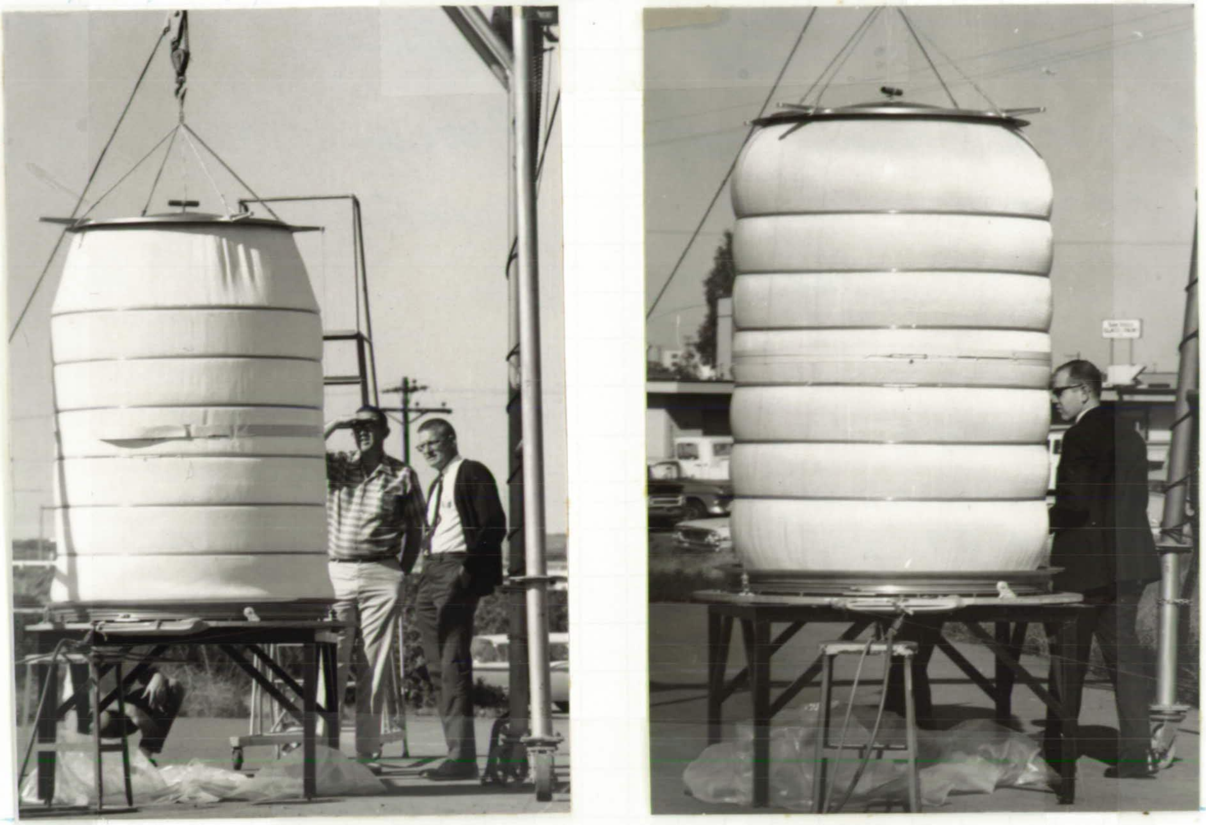

Reduce slightly

Figure 25. First Proof Pressure Test Sequence

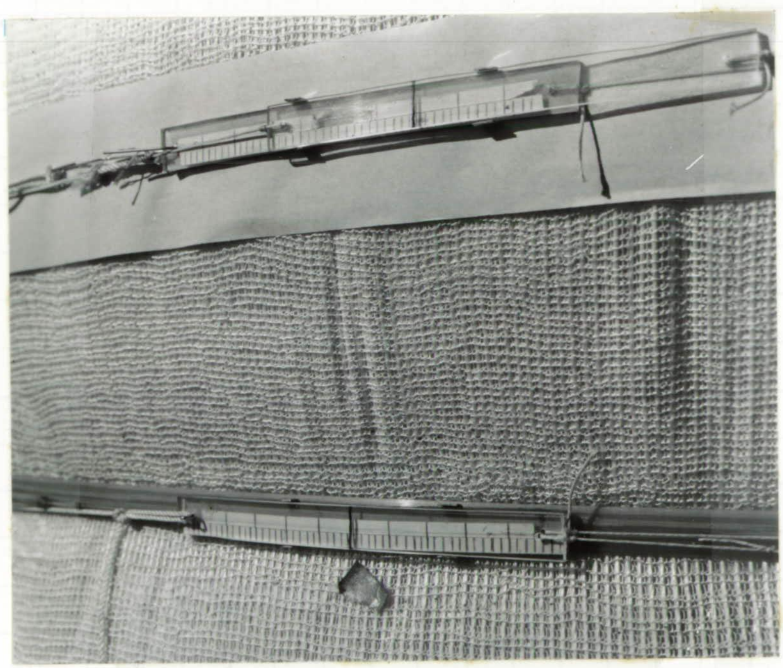

#67-10

Figure 26. Circumferential Strain Instrumentation

R

#67-12
ENLARGE

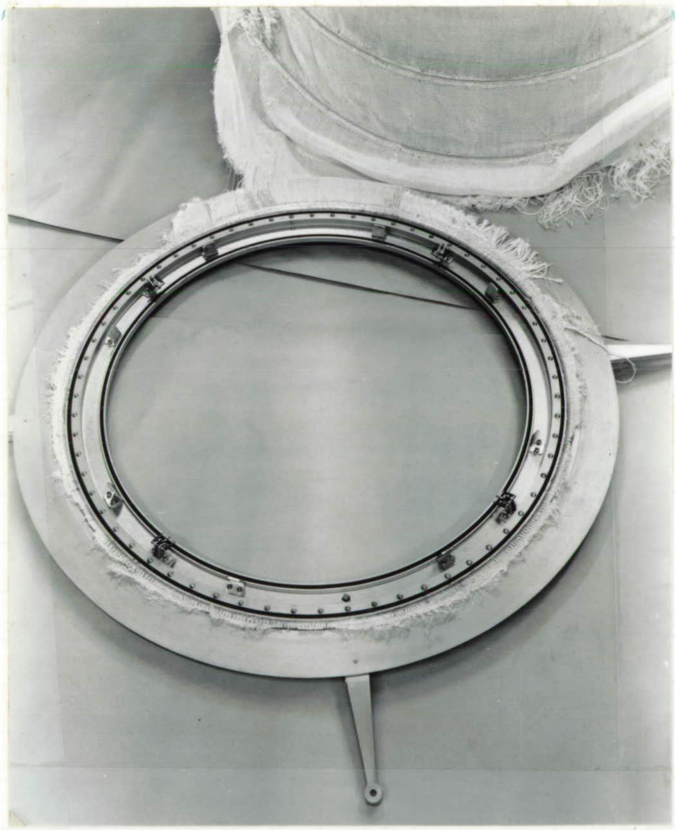

#67-16

Figure 27. Failed Unit of Burst
Pressure of 27.7 psi

(a)

(b)

Figure 28. Structural Cords, Indication of Region of Failure

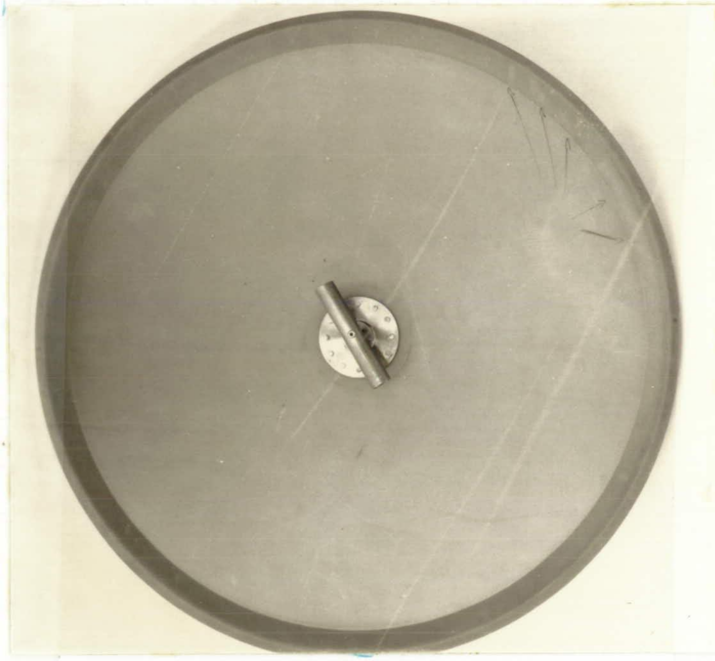

Figure 29. Delaminations in Hatch Rings

Failure Analysis of the First Test Assembly. Investigations were initiated in the following areas, based on potential troublespots:

1. Stress analysis-basic structure.
2. Review of test equipment and test procedure.
3. Evaluation of bolted ring and fixed ring mating tolerances with particular emphasis on the spacing between this bolted ring and the corner existing on the fixed ring.
4. Review of the location of the failure as determined by measurement of the differential in length of the failed longitudinal Dacron fibers.
5. Analysis of the test strain data.
6. Other miscellaneous speculations of potential problem areas.

The stress analysis for the structural fabric was reviewed to ascertain whether or not a variation might have occurred between the actual airlock design and loading, and the predicted strength analysis. The load-carrying filaments were 100-pound test Dacron which showed an average breaking strength of about 88 pounds. Based on an actual count from the airlock model, there were 1,260 longitudinal filaments. The load these filaments must carry is 19,320 pounds for a design pressure of 10 psi. For 50 psi, the loading would be 96,000 pounds. The load per fiber would be 77 pounds. At 28 psi, the total load to be carried by the Dacron fiber is 54,100 pounds, resulting in a load per fiber of 43 pounds. Therefore, the ratio of the average allowable load in the filament to the actual load in the filament at test failure is approximately 2. The fiber failure load at the pressure attained during the test is too low to be attributed to variations in radius of curvature, and other tolerances.

Review was also made of both the test equipment and test procedure; results showed that proper procedure was used and that pressures were applied to the airlock as required.

Since failure occurred at the ring joint, there was a possibility that the ring bolted to the fixed ring "pinched" the fabric in a corner of the fixed ring. A detailed drawing made of this area showed this clearance was sufficient to allow the fabric to pass freely through this area. Actual measurements were also made on the airlock to define the true spacing. Clearance was measured with and without O-rings. Sufficient clearance again was demonstrated.

Examination of the local failure area indicated two predominant characteristics. In areas near the unfailed portion of the upper fabric, the length of the individual filaments to the breaking point were nearly equal. In the area where the failure supposedly started, adjacent filaments showed a differential in length. A study was then conducted to determine the consequences of the differential lengths.

A layout was made of the ring cross-section (Figure 30a). If the fabric failed at the point marked by arrow A, the resulting differential length would be as shown. This differential length was approximately 2.3 inches. The average from a number of measurements for this differential in length was approximately 0.9 inch. The actual fiber breakage point was then evaluated to determine that point at which actual failure occurred. Two points of potential failure resulting from this 0.9 average measured differential are shown in Figure 30(b) as points B and C. Point C coincides with a bearing pressure resulting from the tension in the fabric, expanding the glass ring against the fixed aluminum ring. In Figure 28, photographs of the broken fibers are shown. In Figure 28(b), the broken fibers are of approximately equal length. In Figure 28(a), in the area marked a, the differential is where the 0.9 average differential occurs.

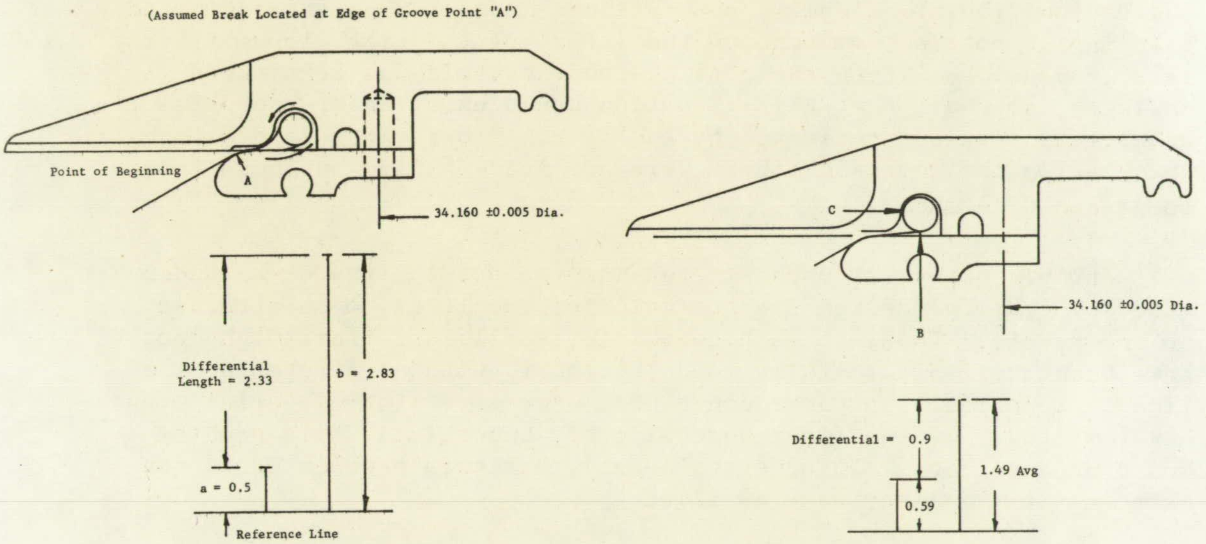

(a) Projected (b) Actual

Figure 30. Projected Fiber Break Length and Actual Fiber Breakage Locations

Various other potential problem areas were examined in this failure analysis, including the lack of uniformity in load in the various Dacron filaments due to differences in length. The bonded bands provides a fixity for the filaments and, therefore, fixes the length of each pair of filaments. It was possible that under pressure these filaments were not capable of elongating sufficiently to provide a uniform loading among filaments. Also, based on the direction in which the fabric pulls the glass-reinforced ring at the joint and based on the stiffness of this ring, it was possible that bearing stresses occurred between the glass ring and the aluminum fixed ring. This pressure would have further caused an unbalance in loading between adjacent fibers in addition to providing normal pressure on the Dacron fibers. Finally, observations made of the part indicated that in the potting compound on the inside of the ring, loose fibers exist, suspended within the potting compound. It was considered unlikely, however, that this situation could exist under the pressure and stress levels experienced by the Dacron fibers when loaded. Speculation that certain fibers were not loaded based on these loose loops could be made.

Another potential problem area was the possibility of an undersized liner. The design did not call for the liner to be attached to the fabric. Thus, at each convolute, sufficient liner might not have been available to fully load the fabric without stretching the liner. Conversely, at some convolutes excessive liner material might have existed. If the liner were slightly undersized, this problem would be amplified. In order to assure that this problem would not exist, a larger liner was installed.

Corrective Action. Three major corrective measures were taken in order to prevent a repetition of failure:

1. Modified End Ring: The end rings, over which the load-carrying cords were looped, were modified by adding grooves into which the cords would recess.

2. Improved String Material: In order to improve the reliability of the load-carrying strings, changes were made in their composition. The new material was Style 73 Dacron yarn, of the following configuration:

Various other potential problem areas were examined in this failure analysis, including the lack of uniformity in load in the various Dacron filaments due to differences in length. The bonded bands provides a fixity for the filaments and, therefore, fixes the length of each pair of filaments. It was possible that under pressure these filaments were not capable of elongating sufficiently to provide a uniform loading among filaments. Also, based on the direction in which the fabric pulls the glass-reinforced ring at the joint and based on the stiffness of this ring, it was possible that bearing stresses occurred between the glass ring and the aluminum fixed ring. This pressure would have further caused an unbalance in loading between adjacent fibers in addition to providing normal pressure on the Dacron fibers. Finally, observations made of the part indicated that in the potting compound on the inside of the ring, loose fibers exist, suspended within the potting compound. It was considered unlikely, however, that this situation could exist under the pressure and stress levels experienced by the Dacron fibers when loaded. Speculation that certain fibers were not loaded based on these loose loops could be made.

Another potential problem area was the possibility of an undersized liner. The design did not call for the liner to be attached to the fabric. Thus, at each convolute, sufficient liner might not have been available to fully load the fabric without stretching the liner. Conversely, at some convolutes excessive liner material might have existed. If the liner were slightly undersized, this problem would be amplified. In order to assure that this problem would not exist, a larger liner was installed.

Corrective Action. Three major corrective measures were taken in order to prevent a repetition of failure:

1. Modified End Ring: The end rings, over which the load-carrying cords were looped, were modified by adding grooves into which the cords would recess.

2. Improved String Material: In order to improve the reliability of the load-carrying strings, changes were made in their composition. The new material was Style 73 Dacron yarn, of the following configuration:

- Six strands of 1100 denier each, twisted into a single cable of 6600 denier.

- 2 by 3 cable, with two strands twisted together, 5.3 turns per inch, and with the three sets of two strand cables twisted together at 2.5 turns per inch.

- Cables hot-stretched to reduce subsequent elongation. No coating application, based on evaluation test data.

The new form of string was selected because of its greater strength and lower degree of elongation.

In addition to increased reliability from the new string material, a study program was initiated jointly by NASA and Whittaker to improve abrasion resistance. Several string coating materials were evaluated under an abrasion fatigue environment. One coating, Goodyear AD 917, did improve the abrasive resistance quality of the strings. However, the process for coating the string, at the time it was required, was not sufficiently developed for the quantities required.

3. Increased Number of Strands: The total number of load-carrying strands was increased to reduce the unit load on each strand. The number later used was 2032, whereas the previous number of strings was 1260.

Improved Fabric Evaluation. A number of tests of string fibers were made which strongly influenced the corrective action taken following the failure of the first proof-test. The results on one series of tests are shown in Table III.

R

TABLE III

FABRIC SPECIMENS TEST RESULTS

Specimen No.	Type Fabric	Number of Strands	Failing Load, lb	Load/Strand, lb	Total Elongation, %
1	Braided (Uncoated)	178	6,100	34.2	11.2
2	Braided (Uncoated)	154	9,000	58.3	16.2
3	Coated	140	11,800	84.3	18.5
4	Uncoated	132	12,500	94.7	11.1

The fixture used in these tests simulated the joint configuration of the actual airlock. However, Specimen 1 was intentionally assembled with more loops than groves, which thereby induced bearing-type loading on some of the loops. The effect of this condition can be noted in Table III and in Figures 31(a) and 31(b), which show the appearance of the specimen after testing. The test fixture is illustrated schematically in Figure 32, while Figure 33 shows the method by which the strands were held so that no bearing load could be applied to the specimen. The test fixture is also illustrated in Figures 34 and 35.

The conclusion reached from the test of Style 73 Dacron fabric was that failure occurred at loads lower than expected, but that the strength margin of safety was still greater than 5. A further conclusion was that the ring grooves should be deepened, a change that was later made.

An additional cycling test was run on an uncoated sample of the original Style 52 Dacron-fabric, with the maximum load equivalent to a proof pressure of 30 psig. The sample was cycled from zero to full load 1000 times and then tested statically. Failure occurred at 98% of the stress at which a similar uncycled sample failed.

Cycling tests were conducted on a sample fabricated of Style 73 Dacron. The load was varied from 0 to 28 pounds per yarn for 1000 cycles. The first yarn of the selvage edge broke at the rod. A similar sample tested statically failed at 10,600 pounds or 74 pound yarn. This is shown in Figure 36. The yarn failures occurred at the rods and were attributed to abrasion of the yarn by the rod. In all of these tests, the sample was judged to have failed when significant eccentricity, caused by strand failures, was observed. This condition can be seen in Figures 36(a) and 36(b). A schematic drawing (NR-351) of the fabric specimen is shown in Figure 37.

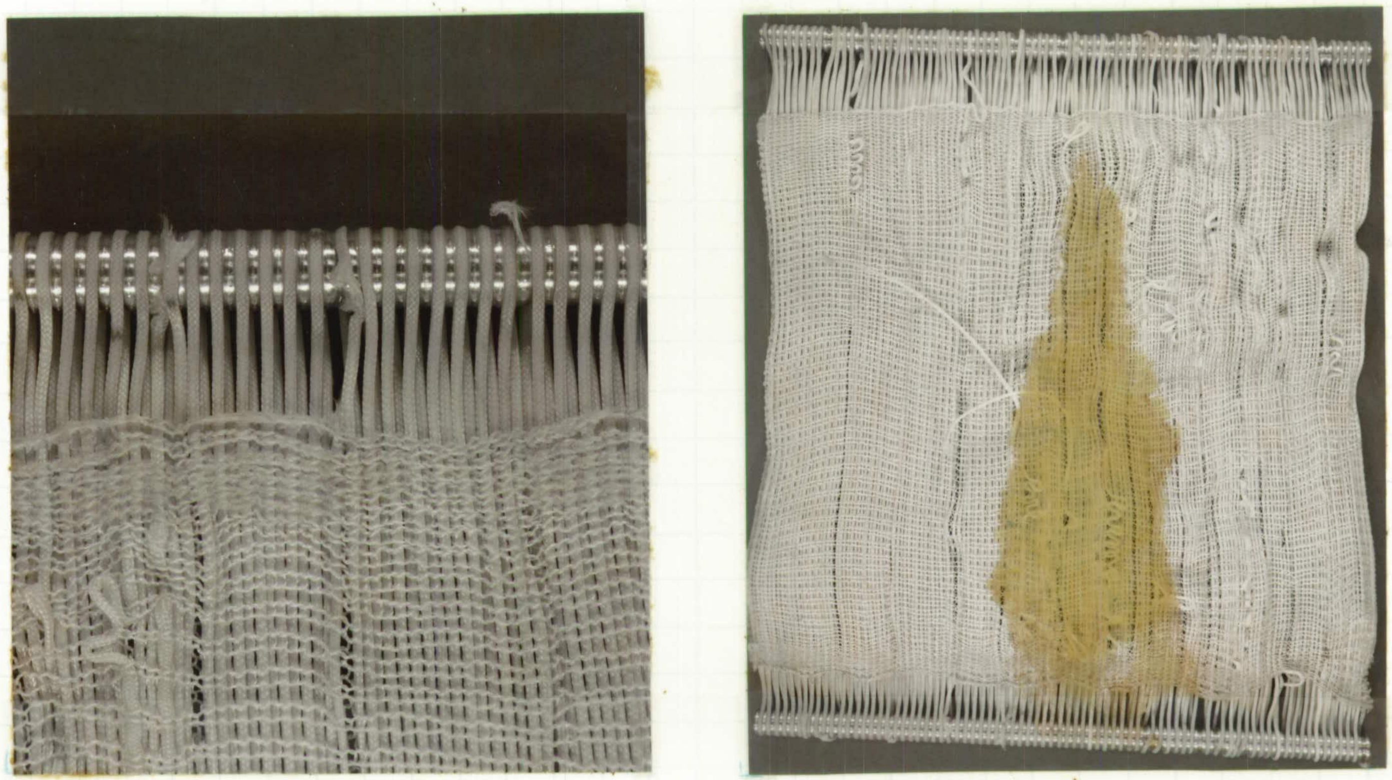

(a) (b)

Figure 31. Fabric Test Specimen, Showing Failures Resulting from Pinched Dacron Cords

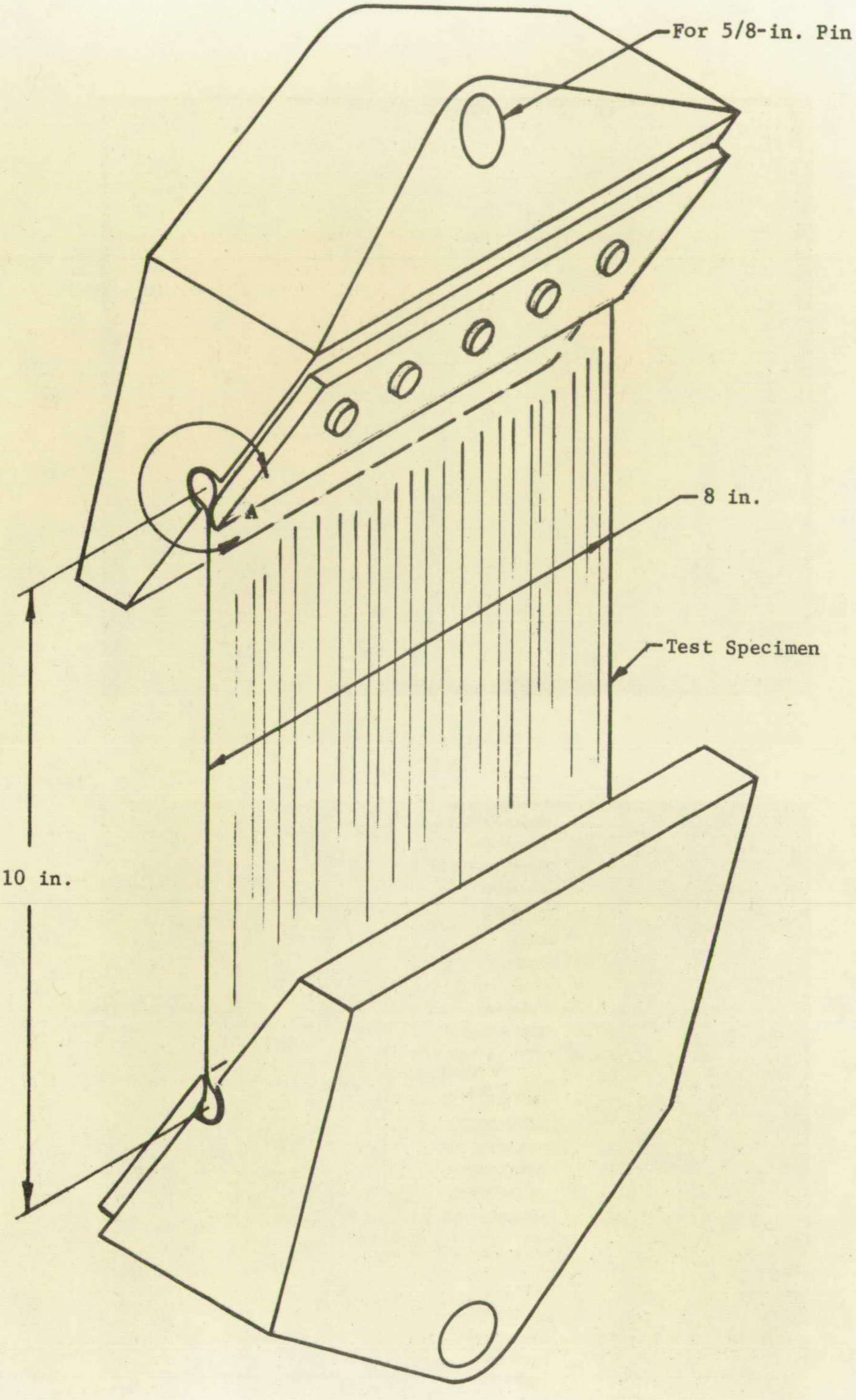

Figure 32. Test Fixture

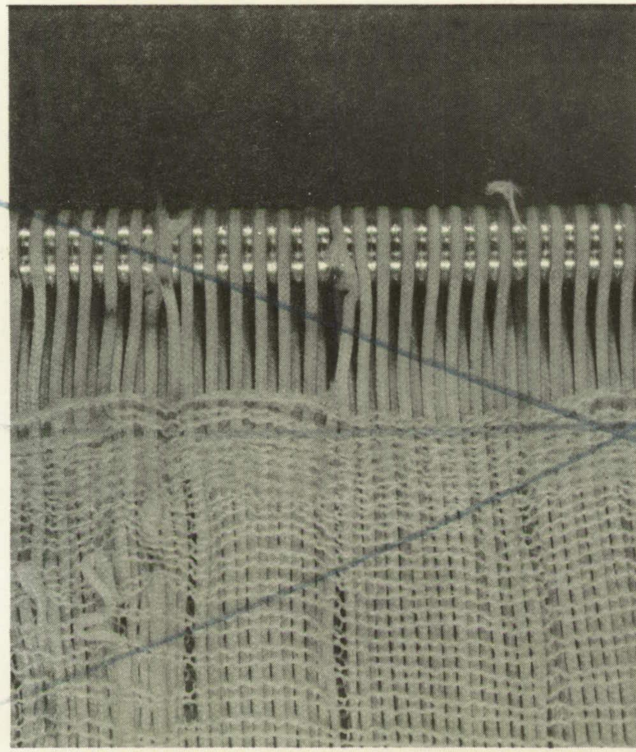

(a)

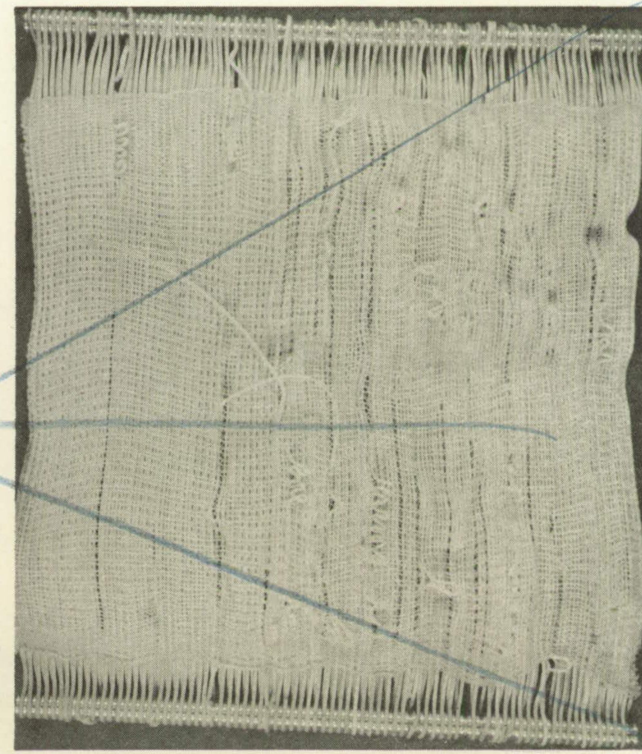

(b)

Figure 31. Fabric Test Specimen, Showing Failures Resulting from Pinched Dacron Cords

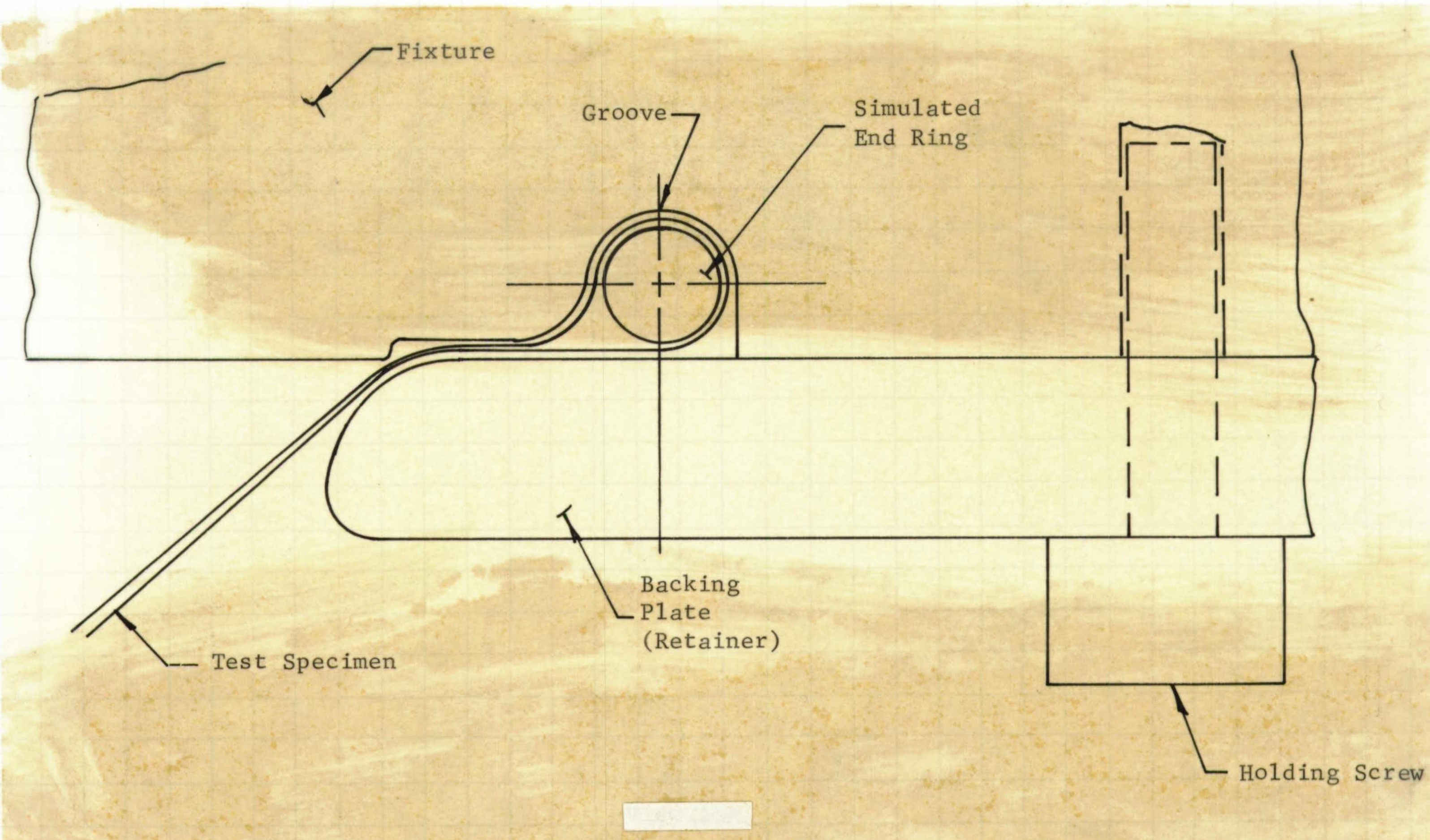

Figure 33. Method of Holding Strands

R

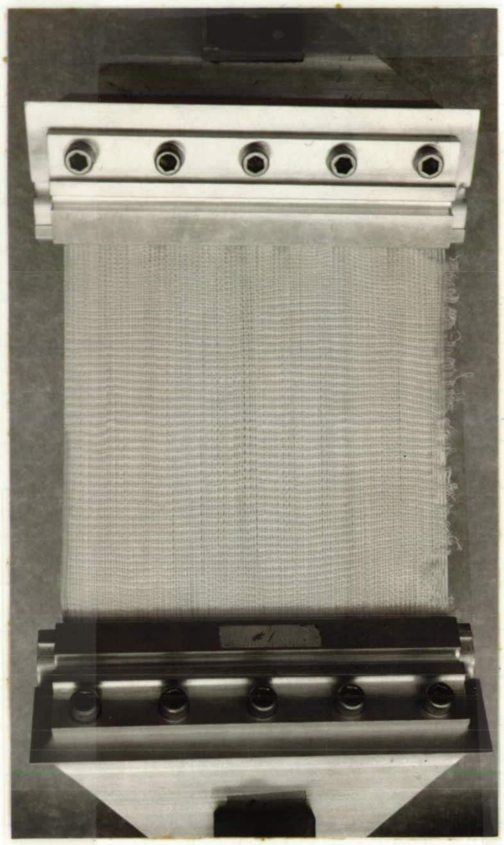

Figure 34. Failure of Fabric Test Specimen after 1000 Cycles

Figure 35. Fabric Test Specimen Test Fixture

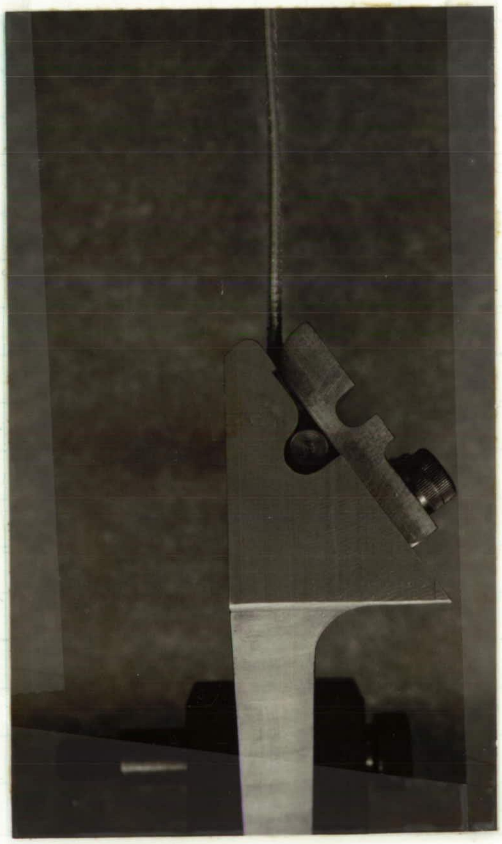

(a)

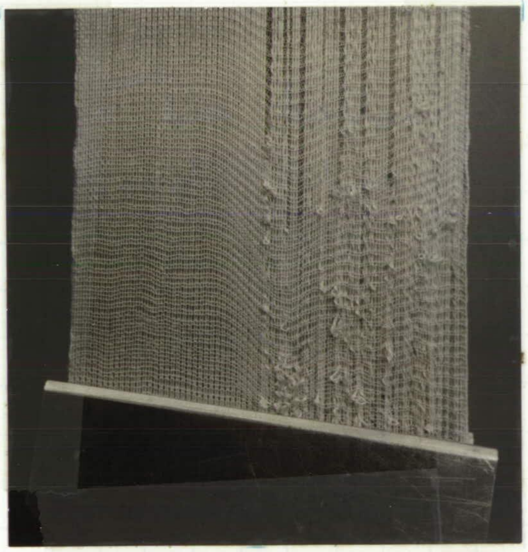

(b)

Figure 36. Grooved End Ring and Fabric Static Strength Test of Style 73 Dacron Fabric

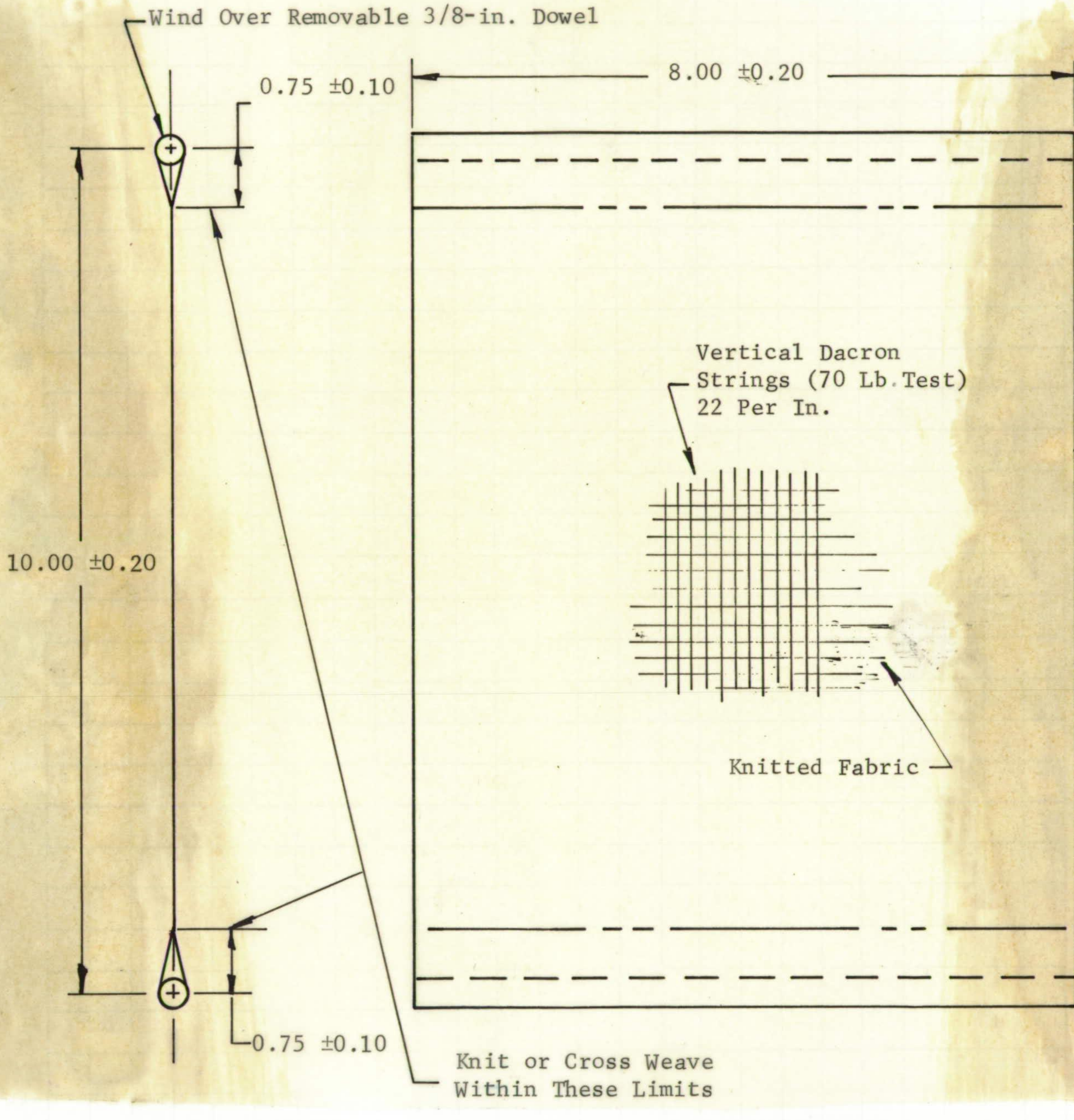

Figure 37. Schematic Diagram of Fabric Specimen

Final Proof Pressure Test

A second proof pressure test of the structural test assembly was conducted on 22 May 1968. The airlock was pressurized from 0 to 29.4 psig with approximately 45 minutes being required to reach full pressure. The full proof pressure of 29.4 psig was maintained for 10 minutes, after which the unit was depressurized. The test was accepted by NASA-LRC as successful. Figure 38 shows the airlock at 29.4 psig proof pressure.

Figure 38. Airlock under Test at 29.4 psig

Retraction Test

Tests of the retracting operation were made, and the results indicated that the mechanism and procedure were satisfactory. The airlock is shown in several stages of retraction in Figure 39.

(a) Retracted

(b) Partially Expanded

(c) Fully Expanded

Figure 39. The Completed Whittaker Expandable Airlock Undergoing Retraction Test

CONCLUDING REMARKS

In conclusion, the contract objectives have been met, in that an airlock has been designed and built to meet all of the stated requirements. However, one problem area remains, that of the buckling of hoop rings during retraction of the airlock. This results from the lack of elongation permitted in the Dacron outer plies of the micrometeoroid barrier. It is recommended that the cloth in the foam laminate be replaced by a cloth comprised of a more flexible material, such as cloth arrayed on the bias.

The following are some of the problem areas encountered during the program. The interface bond between the fiberglass dome and the aluminum end ring must be sufficiently flexible to allow the differential in strain to be accommodated. Through use of a more generous bondline and a more flexible adhesive, this problem was solved.

For handling purposes, a liner which is nearly fully attached to the structural fabric is recommended. Failure to preposition the liner to each convolution results in excess liner in one area and a lack of sufficient liner in another. This imbalance can be corrected manually. The method of attaching the end retainer rings to the structural fabric initially resulted in bearing on the fabric and also in abrasion. Through the use of a stand-off ring, no bearing was permitted on the fabric and reduced the abrasion to a minimum.

Should an uneven length exist in the structural fabric from hoop to hoop, some flexibility in the hoop bond to fabric bond is desirable to help relieve this imbalance. Thus, a more flexible adhesive was used in this adhesive bond.

Blank page only

Page No. only

APPENDIX A

DETAILED TEST PLAN FOR THE EXPANDABLE AIRLOCK

I. PURPOSE

The purpose of this test plan is to present a sequence of tests for the expandable airlock. The test plan is divided into three sections: preliminary acceptance, final acceptance, and system evaluation tests.

II. PRELIMINARY ACCEPTANCE TESTS

The preliminary acceptance tests will be conducted at the Narmco Research & Development facility. Preliminary acceptance will be based upon two test series. The first will be a structural proof pressure test and the second will be an operational check out sequence.

A. Structural Proof Pressure Test

The objective of this test is to demonstrate the structural capabilities of the expandable airlock. Secondary objectives will be to check the seating of the hatch seals and tightness of the liner.

1. Expandable Airlock Components

   The proof pressure test will be performed upon the primary load carrying portions of the airlock. The airlock test unit includes the structural fabric, airlock hatch assembly, base closure plate, retainer rings, liner, and necessary seals. The elastic recovery layers will not be applied to the structural fabric at this time.

2. Test Sequence

   a. The assembled airlock will be placed in the vertical position with the hatch ring supported in the expanded position.

   b. The hatch will be in the seated position (closed) and hatch valve closed for the test.

   c. The airlock assembly will be pressurized to an internal proof pressure differential of 2.0 atmospheres (29.4 psig). The pressurization rate will be approximately 3 psi/min.

A

d. The pressure will be maintained for 30 seconds* then the air valve slowly opens to release pressure.

3. Measurements and Post Test Inspection

a. Measurements of the length, circumference at a hoop band, and circumference at a maximum point on the convolution will be taken during the test.

b. The measurement will be taken at 5 psig intervals.

c. A post test inspection will be made of the airlock to determine the effect of the pressure test on the structural portion of the airlock. Particular items to be inspected include excessive distortions and shifting of the structural fabric, evidence of excessive deformation in the hatch or end rings, and local yielding of the structural fabric in the vicinity of the retainer rings. A secondary inspection will be made of the seals to ascertain the effectiveness of the design for maintaining the pressure.

d. Preliminary acceptance will be made based upon the demonstration the airlock structure withstood the proof pressure without exhibiting the items listed in 3 c. above.

B. System Checkout Test

The objective of this test series is to demonstrate the operation of the various components of expandable airlock system.

1. Expandable Airlock Components

The completed, assembled airlock system will be used for this test sequence.

2. Test Sequence

a. The airlock will be mounted in the vertical direction.

b. Hatch latch operation to be demonstrated by opening and closing the hatch.

c. Hatch valve operation will be demonstrated by opening and closing.

d. Demonstration of the retraction mechanism.

---

* This requirement changed to 10 minutes.

2

(1) The motor controller will be connected to 115 v AC power.

(2) The length of the expanded airlock will be recorded.

(3) The drive unit will be started and the retraction cycle initiated. The retraction speed will be gaged to take approximately one minute.

(4) The retracted length will be measured.

(5) The drive unit will be turned off and the holding or restraining power of the retraction mechanism will be noted.

(6) The drive unit will be reversed and the deployment of the airlock will be monitored. The drive unit speed will be monitored to prevent the cables from becoming slack.

(7) After the deployment cycle of the airlock is complete, the length will be remeasured.

3. Successful completion of the operational sequence will indicate the proper and satisfactory operation of the expandable airlock system.

III. FINAL ACCEPTANCE TESTS

The final acceptance tests will be performed at the NASA-Langley Research Center. The purpose of this test series is to assess the effectiveness of the airlock design. Emphasis will be placed upon the operational characteristics of the airlock system in the vacuum environment. The test series will include structural, operational, and leakage tests.

The following sequence is suggested by Narmco as a guide for performing this test series, however, the details as to equipment availability and operation is not presented due to lack of information on NASA test operations. Narmco personnel will be available during this test series to supervise the airlock assembly into the environmental test chamber.

A. Airlock Assembly

The airlock will be reassembled on the base closure plate as outlined in the report on assembly, handling, and operation of the expandable airlock system.

B. Systems Operational Evaluation

The proper operation of the various systems will be determined.

1. The opening and closing of the airlock hatch will be performed to assure the proper operation of the hatch latch and seal.

2. The hatch valve operation will be checked.

3. The retraction mechanism will be observed as the airlock is retracted.

4. The retraction mechanism will be reversed and the deployment characteristics of the airlock noted.

5. The airlock system will be thoroughly inspected after this series of tests.

C. Structural Evaluation

The structural integrity of the expandable airlock structure will be determined by a pressure test.

1. The completely assembled airlock system will be used.

2. The airlock will be tested outside the environmental test chamber.

3. The airlock will be pressurized to 2.0 atmospheres (29.4 psig) internal gage pressure, at a rate of approximately 3 psi/min.

    a. The length of the airlock will be monitored during the test. Measurement to be taken at 5 psi increments.

    b. The pressure of 2.0 atmospheres to be maintained for one minute.

    c. The pressure will be slowly released through the base valve.

4. The airlock will be thoroughly inspected for evidence of abnormal deformations or straining in the structure.

D. Leakage Evaluation

This test will determine the initial leakage rate of the airlock system.

1. The airlock will be installed in the environmental test chamber for the test.

   a. The retraction drive unit will be removed for this initial test sequence.

   b. The airlock unit will be installed horizontally in the chamber.

2. The environmental test chamber will be pumped to 10^{-6} torr.

3. After the vacuum has stabilized due to any initial outgassing of the elastic recovery materials, the leakage measurement will commence.

4. The initial leakage rate will be established for the airlock system. Final acceptance of the airlock system will be based upon a leakage rate equivalent to no more than 0.2 pounds per 24-hour period at a test pressure of 10^{-6} torr.

IV. AIRLOCK SYSTEM EVALUATION

The objective of the following outline is to suggest a possible continuing expandable airlock system evaluation. This study would indicate to NASA the design features of the expandable airlock which would lead to a man-rated flight article for future space stations. Many of the suggested areas of evaluation have been performed upon rigid airlock systems, hence, would allow for an overall system effectiveness evaluation.

A. Leakage Tests of the Expandable Airlock Components

1. Leakage rates would be established for the various components of the expandable airlock system. The various areas of the airlock would be isolated and area leakage rates would be established. Areas to be considered would include:

   a. Elastic Recovery Wall

      This test would determine the leakage rate for the removable liner.

   b. Total hatch and seal area

   c. Hatch valve leak rate

   d. Base ring leak rate

2. Establish leakage rates for the airlock system after simulated service.

a. Determine the effect of opening and closing hatch 25 cycles upon the leakage rate of the seal.

b. Repeat the hatch seal leakage rate determination after 50 opening and closing cycles.

c. Cycle the hatch valve 50 times and determine any change in leakage rate.

d. Determine the effect of multiple retraction-development cycles upon the leakage rate of the airlock system.

(1) The airlock structure be cycled 50 times. One-half of the cycles be accomplished with a vacuum inside and outside the airlock to simulate operation in a space environment.

(2) The leakage be established at the completion of the deployment cycles.

B. Simulated Egress Evaluation

The objective of these test series would be to determine the effectiveness in which a pressure-suited person could exit through the airlock hatch. The evaluation could include:

1. Valve opening

2. Hatch opening and stowing

3. Egress through hatch

4. Hatch closing

5. Returning through airlock by opening hatch and stowing

6. Ingressing through hatch

7. Closing hatch

A further evaluation would be to repeat the above series of tests in an aircraft flying a parabolic trajectory to simulate an "0 g" environment.

C. Design Review

At the completion of the system evaluation, the tests should be correlated and recommendations agreed to which would upgrade the expandable airlock to a man-rated system.

APPENDIX B

FLEXIBLE STRUCTURE ANALYSIS

I. DESIGN SPECIFICATIONS

A. General Considerations

The airlock structure is to be fabricated so as to have the size and shape described in Figure 2, at the working pressure of one atmosphere. The ends of the chamber are to be closed by end plates, to which the end rings will be clamped. The pressure liner is to be a tailored rubberized-fabric bag; and the whole structure is to be covered with a multiple-layer meteoroid bumper, the inner layer of which is a 0.3-inch thick sheet of flexible foam. This foam layer is to be bonded to the Airlock structure in such a way that it promises to act as a controlling "matrix" for the flexible structure. In addition, the meteoroid bumper uses two layers to tightly-woven Dacron cloth which will constrain the folding deformations of the structure to some sort of isometric wrinkling.

B. Performance Requirements

1. Working pressure: 14.7 psig

The structure is to have the prescribed geometry and dimensions at this working pressure.

2. Proof pressure: 29.4 psig

The structure is to be subjected to this pressure during the acceptance testing. No time limit or number of cycles has been specified.

3. Burst pressure: 50 psig

This pressure has been established in order to define the margin of safety. It is not known whether the structure will be tested at this pressure. This requirement has been taken as the designing condition.

4. Repeated load: 0 to 14.7 psig for 1000 cycles

This requirement was included to insure reliability.

C. Properties of Materials

1. Hoops and End Rings:

Material	S-glass roving, 20-end, with B-stage epoxy prepreg.
Ultimate strength of composite	assumed 200,000 $lb/in.^2$ (6.0 lb/end)*
Modulus of elasticity of composite	7.5×10^6 $lb/in.^2$ (Ref. 2)
Density of composite	0.077 $lb/in.^3$
Specific strength	2.5×10^6 in.
Ultimate elongation	$\frac{200{,}000 \text{ psi}}{7.5 \times 10^6 \text{psi}} = 0.0267$ in./in.

2. Longitudinal Fiber:

Material	Dacron, heat-stretched, twisted roving, 6300 denier (100-lb-test nominal)
Ultimate strength	80 lb with simulated end-ring clamp (93 lb with single-fiber test)
Specific strength	2.0×10^6 in.

3. Knitting Matrix:

Material	Nylon sewing thread, size "B" (9800 yds/lb = 380 denier) 5.6-lb test nominal

---

* Measured strength in one NOL-ring test - 220,000 $lb/in.^2$

II. DESIGN CALCULATIONS

A. Basic Loads Analysis

In the loads analysis presented in Reference 1, the designing condition which was used was that the stress in the various members at the working pressure was to be a fixed fraction of the ultimate stress for each material. This approach permitted the members to be designed directly from an analysis of the working loads in each member. Thus the structure of Reference 3 is designed to have a stress of 20 percent of the ultimate at the working pressure of 10 psi.

The requirements of the contract under which the present work is being done, however, are such that this approach is not adequate; in order to design for the prescribed burst condition, the deformation of the structure under load must be considered. This process is complicated here by the requirement that the structure must have the prescribed dimensions at the working pressure. Since the stress at the working pressure is not known, the increase in strain from working pressure to burst pressure is unknown, and the size at burst is therefore unknown. This problem may be solved iteratively by assuming a working strain, computing the growth to burst, computing the required member sizes, and then recomputing the stress and strain at the working pressure to make another approximation. For the problem at hand, however, convergence is sufficiently rapid that the first try gives the desired accuracy.

To simplify the calculation, it will be assumed that the growth in the longitudinal direction is determined by the strain in the longitudinal Dacrom fibers alone, while the radial growth is determined only by the strain in the fiberglass hoops. The load in the longitudinal fibers at burst is then

$$nT^* = p^* \pi\, r_o^{*2} = p^* \pi\, r_o^2\, (1+\Delta\epsilon_R^*)^2 \qquad (1)$$

---

* indicates burst condition; quantities without * are conditions at working pressure.

where p = pressure

T = tension in each of n longitudinal fibers

r_o = outside radius of convolution

$\Delta\epsilon_R$ = change in radial strain from working-pressure condition

Now the ratio of working pressure to burst pressure is

$$\frac{p}{p^*} = \frac{14.7 \text{ psi}}{50 \text{ psi}} = 0.294$$

To allow for some expansion, assume that the working stress of the glass is 0.25 of the ultimate stress. Further assume a linear stress vs strain curve. Then

$$\epsilon_{R_{working}} = 0.25\ \epsilon_R^*$$

and

$$\Delta\epsilon_R^* = \epsilon_R^* - \epsilon_{R_{working}} = 0.75\ \epsilon_R^*$$

For the hoop material, $\epsilon_R^* = 0.0267$ (see Sec. I-C).

Therefore

$$\Delta\epsilon_R^* = 0.75\ (0.0267) = 0.020$$

For $r_o = 24.00$ in. and $p^* = 50$ psi, then Equation (1) gives

$$nT^* = 101{,}000 \text{ lb.}$$

If we take $T^* = 80$ lb, then

$$n = 1260 \text{ fibers.}$$

The working tension in the fibers is given by

$$T = \frac{p \pi r_o^2}{n}$$

For $p = 14.7$ psi, then $T = 22.6$ lb. From tests made on the fiber at this tension level, it has been found that a working strain of 3.0 percent must be allowed for (this is the strain in the fiber at a tension of 22 lb after a proof load of 45 lb has been applied for several hours). For an ultimate strain of 7.0 percent, then, the strain increment in the longitudinal direction at burst is

$$\Delta\epsilon_L^* = 0.040.$$

To compute the hoop tension at burst, it is convenient to express the hoop force in terms of the dimensions of an equivalent cylinder having the length of one convolution. Thus

$$T_H = p \cdot 2Z_H \cdot \bar{r} \qquad (2)$$

where $2Z_H$ = convolution length = 8.80 in.

$\bar{r}$ = mean radius.

To find $\bar{r}$, note that the convolution arc may be approximated by a parabola. Then

$$\bar{r} \cong \frac{2r_o + r_H}{3} = 24.57 \text{ in.}$$

B

Now

$$\bar{r}^* = \bar{r}\,(1 + \Delta\epsilon_R^*)$$

and (3)

$$Z_H^* = Z_H(1 + \Delta\epsilon_L^*)$$

Therefore the hoop tension at burst, from Eq. (2) is

$$T_H^* = p^* \cdot 2Z_H \quad (1 + \Delta\epsilon_R^*)\,(1 + \Delta\epsilon_L^*)$$

For the values which have been determined,

$$T_H^* = (50)\,(8.80)\,(24.57)\,(1.02)\,(1.04) = 11{,}500 \text{ lb.}$$

With an allowable stress of 200,000 lb/in.^{2}, this requires an area of

$$A_H = \frac{11{,}500}{200{,}000} = 0.0575 \text{ in.}^2.$$

At a working pressure of 14.7 psi, the hoop tension is

$$T_H = 14.7\,(8.80)\,(24.57) = 3190 \text{ lb.}$$

This gives for the strain ratio

$$\frac{\epsilon_R}{\epsilon_R^*} = \frac{T_H}{T_H^*} = \frac{3190}{11{,}500} = 27.7 \text{ percent.}$$

This value is sufficiently close to the original assumption of 25 percent to make a second iteration unnecessary. Thus the loads as computed above are considered adequate for this large-deformation analysis.

B. Detail Design Calculations

1. Hoops

a. Cross-section detail:

From the preceding section, design load at burst is

$$T_H^* = 11{,}500 \text{ lb}$$

Ultimate stress is taken to be

$$S_{ult} = 200{,}000 \text{ lb}$$

Cross-section area is therefore

$$A_H = \frac{T_K^*}{S_{ult}} = \frac{11{,}500}{200{,}000} = 0.0575 \text{ in.}^2$$

At 6.0 lb/end, or 120 lb/turn, this requires 96 turns (say 100).

b. Diameter:

For working stress of 27 percent of ultimate, the strain at the working load is

$$\epsilon_R = 0.27\ (0.0267) = 0.0072$$

For a radius of 24 in., this is a radius change of $\Delta r = 0.17$ in.

The inside diameter of the ring at working pressure is then

$$ID_{work} = 2(24.00 + 0.034) = 48.07$$

The relaxed diameter is smaller by the amount of the working elongation:

$$ID_{relaxed} = 2(24.00 + 0.034 - 0.17) = 47.73$$

The mandrel diameter should be from 0 to 0.0005 in./in. less than the ring diameter since the ring tends to be oversize by about that amount. This gives a probable expansion of 0.01 in. The mandrel diameter should therefore be

$$\text{Diameter mandrel} = 47.72 \text{ in.}$$

2. End Rings

a. Cross-section detail:

The ring cross section is required to be circular because of the details of the mechanical design. Furthermore, the design provides for supporting the end ring in a groove in a heavy plate, thereby preventing it from elongating. This ring, as presently conceived, therefore does not carry the radial load of the longitudinal fibers. It has been decided, however, to design and build the ring with the capability of carrying the end-ring load without support from the end plates.

The end-ring load is given in Reference 3 as

$$T_D = \frac{nT}{2\pi} .$$

For the burst condition, from Section II-A,

$$nT^* = 101{,}000 \text{ lb}$$

Therefore, the burst condition for the end ring is

$$T_D^* = \frac{101{,}000}{2\pi} = 16{,}100 \text{ lb}$$

For an ultimate stress of 200,000 lb/in^2, the cross-section area must be

$$A_D = \frac{16,100}{200,000} = 0.081 \text{ in.}^2$$

This corresponds to a circle of 0.322 in. diam. to allow a margin for hand-working the cross section; call this

diam. cross section = 0.33 in.

b. Diameter:

The end ring is required to fit in a groove in the end plate. The mean diameter of the ring without load (during assembly) is to be 36.00 in. Since the ring is to be made so that it will be no smaller than this nominal diameter, the mandrel diameter should be based on the assumption that no expansion will occur. The mandrel ID is therefore 35.67 in.

c. Assembly of end ring and retainer:

The retainer ring which is used to clamp the end ring in place must be placed inside the airlock structure. It is of interest to determine whether the end ring is capable of being spread enough to allow the retainer to be inserted after assembly of the structure. The following calculation shows that this can be accomplished without danger of breaking the end ring.

From Roark (Ref. 4) Table VIII, Formula 1, for a slender ring loaded at two points on a diameter, the change in diameter at the load, W , is given as

$$\Delta D_y = 0.149 \frac{WR^3}{EI}$$

The maximum bending moment occurs at the loading points and is given by

$$M = 0.318\ WR$$

By solving each of these relations for W and then substituting $S = \frac{Mr}{I}$ for M , it is possible to solve for the stress, S , at the point of maximum moment in terms of the diameter change. The result is

$$S = 2.13\ \frac{Er\Delta D_y}{R^2}$$

Here the ID of the end ring is 35.67 in., while the OD of the retainer ring is 37.86. The required diameter change is therefore

$$\Delta D_y = 37.86 - 35.67 = 2.19 \text{ in.}$$

Also

$$E = 7.5 \times 10^6 \text{ lb/in}^2$$

$$r = 0.33/2 = 0.165$$

$$R = 18.00$$

These values give $S = 18{,}000$ psi. The required load, W , is found to be

$$W = \frac{\Delta D_y\ EI}{0.149\ R^3} = 11 \text{ lb}$$

3. Longitudinal Fibers

a. Number of fibers:

In Section II-A the total load, at burst, in the longitudinal structure was found to be

$$nT^* = 101,000 \text{ lb.}$$

For a breaking load of 80 lb per fiber, this gives

$$n = 1260 \text{ fibers.}$$

At the diameter of the hoops, the spacing of these fibers is 8.3 per inch, while at the diameter of the end rings, the spacing is 11.1 per inch.

b. Free length of fibers:

It is assumed that the structure is to have the prescribed geometry at the working pressure, after having been subjected to the proof pressure. From tests of the fiber it has been determined that the elongation for this condition is 3.0 percent. The free length can then be determined as follows:

Working length of theoretical curve	81.85
Correction for end detail, both ends	0.50
	82.35

This length is 3.0 percent greater than the free length. Thus

$$\text{free length} = \frac{82.35}{1.03} = 79.95 \text{ in.}$$

For the purpose of marking the string at the hoop stations, this length may be divided as follows:

	Increment	Total
End ring		0
	18.15	
First hoop		18.15
	8.73	
Second hoop		26.88
	8.73	
Third hoop		35.61
	8.73	
Fourth hoop		44.34
	8.73	
Fifth hoop		53.07
	8.73	
Sixth hoop		61.80
	18.15	
End ring		79.95

4. Knitting Matrix

The knitting sheet which forms the body of the Airlock structural surface is made using two rows of knit-and-purl stitches for each string. This texture was chosen on the basis of a number of samples made to try various combinations of stitch geometry and knitting tension.

APPENDIX C

HATCH ANALYSIS

1. Material Properties

Assume an eight ply laminate (181 style cloth, epoxy resin) with the plies oriented as shown below.

Numbers indicate ply number, arrows indicate warp direction

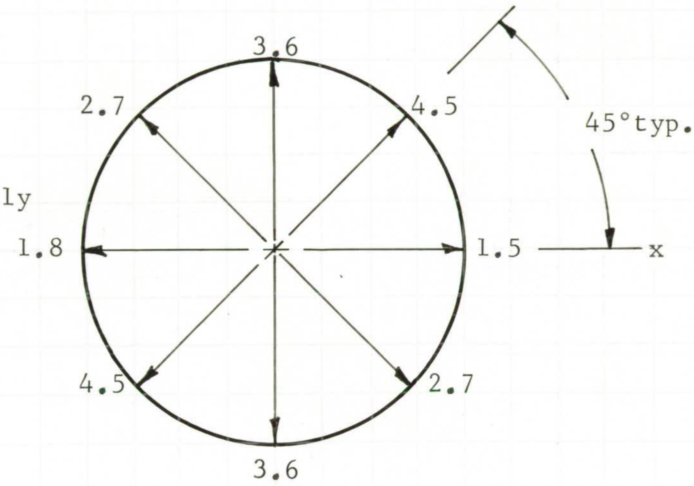

Then, from MIL-HDBK-17, in the x direction

Ply No.	F_{tu} psi $\times 10^3$	E psi $\times 10^6$	$\epsilon_a = F_{tu}/\epsilon$ $\times 10^{-3}$
1	44	3.1	14.19
2	27	2.2	12.27
3	42	2.9	14.48
4	27	2.2	12.27
5	27	2.2	12.27
6	42	2.9	14.48
7	27	2.2	12.27
8	44	3.1	14.19

where F_{tu} = Ultimate tensile strength, psi

E = Modulus of elasticity, psi

ϵ_a = Allowable strain, in./in.

The allowable strain for the laminate is

$$\epsilon_{a_{min}} = 12.27 \times 10^{-3} \text{ in./in.}$$

The average modulus of the laminate is

$$E = \frac{\Sigma E_n}{n} = 2.60 \times 10^6 \text{ psi}$$

Therefore, the allowable tensile strength of the laminate is

$$F_a = \epsilon_a \epsilon = (12.27 \times 10^{-3})(2.60 \times 10^6) = 31.9 \times 10^3 \text{ psi}$$

2. <u>Pressure Load</u>

The thickness of each ply is $t_n = 0.0085$ in. The total thickness of the laminate is

$$t = nt_n = 8(0.0085) = 0.068 \text{ in.}$$

The tensile stress in a spherical dome subjected to internal pressure is

$$f_t = \frac{pa}{2t} \qquad (1)$$

where f_t = Membrane tensile stress

a = Spherical radius

p = Internal pressure

$$f_t = \frac{50(35.70)}{2(0.068)} = 13.13 \times 10^3 \text{ psi}$$

The margin of safety is

$$\text{M. S.} = \frac{31.90}{13.13} - 1 = +1.43$$

3. Discontinuity at Edge of Dome

Equation (1) gives only the membrane stresses. At the edge of the dome the aluminum ring causes discontinuity stresses which must be superimposed upon these membrane stresses. The configuration in this area is shown in the sketch below.

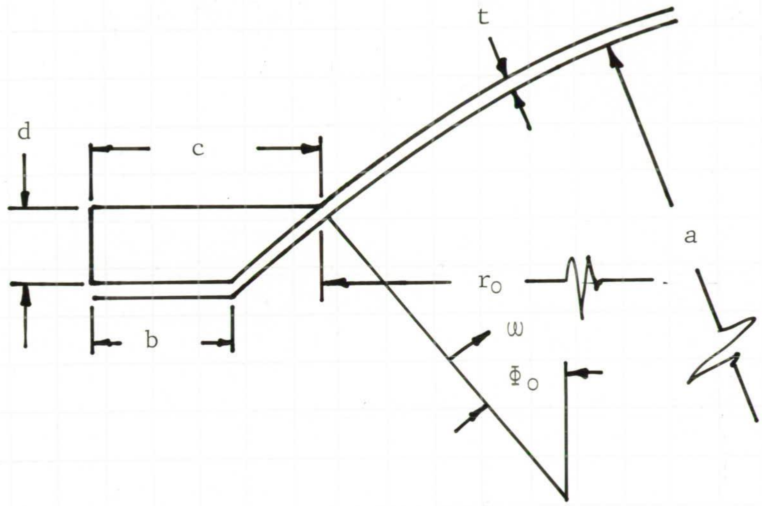

For simplicity, the portion of the laminate which is wrapped around the ring will be neglected.

From Timoshenko*,

$$\delta_o = \frac{r_o}{E_1 t} \left(N_\theta - \mu N_\Phi\right) \tag{2}$$

$$V_o = \frac{1}{E_1 t} \cot \Phi_o \; (1 + \mu)(N_\theta - N_\Phi) \tag{3}$$

$$H_o = -\cos \Phi_o \; (N_\Phi) \tag{4}$$

$$\delta_1 = \frac{H_o r_o^2}{E_2 \, d\left(\frac{b + c}{2}\right)} \tag{5}$$

$$\delta = \frac{2\lambda^2 \sin \Phi_o}{E_1 t} M - \frac{2a\lambda \sin^2 \Phi_o}{E_1 t} H \tag{6}$$

$$V = -\frac{4\lambda^3}{E_1 ta} M + \frac{2\lambda^2 \sin \Phi_o}{E_1 t} H \tag{7}$$

$$\delta_2 = \frac{Hr_o^2}{E_2 \, d\left(\frac{b + c}{2}\right)} \tag{8}$$

$$V_2 = \frac{r_o^2}{E_2 \frac{d^3 (c^2 + 4cb + b^2)}{36(c + b)}} [M + He] \tag{9}$$

where

N_Φ , N_θ = Membrane loads in meridianal direction and direction perpendicular to meridian, respectively

μ = Poisson's ratio of dome

δ_o = Radial deflection of dome at $\omega = 0$ due to N_Φ and N_θ

V_o = Rotation of edge tangent of dome due to N_Φ and N_θ

H_o = Horizontal thrust on ring caused by N_Φ

δ_1 = Radial deflection of ring due to H_o

M , H = Moment and radial load to ring and edge of dome for compatibility of dome and ring deflection and rotation

λ^4 = $3(1 - \mu^2)(a/t)^2$

δ = Radial deflection of dome edge due to M_α and H

V = Rotation of dome edge due to M_α and H

δ_2 = Radial deflection of ring due to H

V_2 = Rotation of ring due to M_α and H

E_1 = Modulus of elasticity of dome

E_2 = Modulus of elasticity of ring

e = Distance from ring centroid to point of application of H = $\frac{d(c + 2b)}{3(c + b)}$

Then, for displacement and rotation compatability

$$\delta_{\Theta} + \delta = \delta_1 + \delta_2 + V_2 e \tag{10}$$

$$V_0 + V = V_2 \tag{11}$$

Substituting the values,

$$\begin{aligned}
N_\theta &= N_\Phi = \frac{pa}{2} = 892.5 \text{ lb/in.} \\
\mu &= 0.12 \\
E_1 &= 2.60 \times 10^6 \text{ psi} \\
E_2 &= 10.0 \times 10^6 \text{ psi} \\
r_{\Theta} &= 13.987 \text{ in.} \\
\Phi_{\Theta} &= \sin^{-1} r_{\Theta}/a = 23°04' \\
\alpha &= 0.45 \text{ in.} \\
b &= 0.50 \text{ in.} \\
c &= 1.513 \text{ in.} \\
t &= 0.068 \text{ in.} \\
e &= 0.1872 \text{ in.}
\end{aligned}$$

into equations (2) through (9) results in

$$\begin{aligned}
\delta_{\Theta} &= 0.062135 \text{ in.} \\
V_0 &= 0 \\
H_{\Theta} &= -821.145 \text{ lb/in.} \\
\delta_1 &= -0.03546 \text{ in.} \\
\delta &= 0.004001\ M - 0.001863\ H \\
V &= -0.017190\ M + 0.004001\ H \\
\delta_2 &= 0.0000432\ H \\
V_2 &= 0.002796\ M + 0.000524\ H
\end{aligned}$$

Substituting these values into equations (10) and (11) results in two simultaneous equations with M and H as the only unknowns.

$$\begin{aligned}
3.479\ M - 2.004\ H &= -97.600 \\
-19.986\ M + 3.477\ H &= 0
\end{aligned}$$

Solving,

$$M = 12.137 \text{ in.-lb/in.}$$
$$H = 69.77 \text{ lb/in.}$$

Then

$$\delta = -0.08142 \text{ in.}$$
$$V = 0.07050 \text{ radians}$$
$$\delta_2 = 0.003014 \text{ in.}$$
$$V_2 = 0.07050 \text{ radians}$$

The total deflection at the dome edge is

$$\delta_o + \delta = -0.0193 \text{ in.}$$

and the rotation at the edge is

$$V_o + V = 0.0705 \text{ radians} = 4.04°$$

The bending moment in the dome, at some distance from the edge of the dome, is given by[6]

$$M_{\Phi} = \frac{a}{\lambda\sqrt{2}}\, c e^{-\lambda\omega} \sin\left(\lambda\omega + \gamma + \frac{\pi}{4}\right) \tag{12}$$

For the edge condition $(\omega = 0)$ of $M_{\Phi} = M$ and $N_{\Phi} = 0$ the required constants are

$$\gamma = 0 \quad , \quad c = \frac{M\,2\lambda}{a}$$

and equation (12) reduces to

$$\left(M_{\Phi}\right)_1 = \sqrt{2}\, M\, e^{-\lambda\omega} \left(\sin \lambda\omega + \frac{\pi}{4}\right) \tag{13}$$

For the edge condition of $M_\Phi = 0$ amd $N_\Phi = -H \cos \Phi_o$, $\gamma = -\frac{\pi}{4}$ and $c = -\frac{2H \sin \Phi_o}{\sqrt{2}}$

Then, equation (12) becomes

$$\left(M_\Phi\right)_2 = -\frac{a}{\lambda} H \sin \Phi_o \; e^{-\lambda\omega} \sin \lambda\omega \qquad (14)$$

Combining equation (13) and (14)

$$M_\Phi = e^{-\lambda\omega}\left[\sqrt{2}\; M \sin\left(\lambda\omega + \frac{\pi}{4}\right) - \frac{a}{\lambda} H \sin \Phi_o \sin \lambda\omega\right] \qquad (15)$$

where e = Naperian logarithmic base

With the previously calculated values for the parameters in equation (15),

M = 12.137 in-lb/in.

H = 69.77 lb/in.

a = 35.70 in.

λ = 30.046

Φ_o = 23° 04'

The value of M_Φ can be calculated for any value of ω . Values of M_Φ (meridional bending moment in hatch dome) for values of ω from 1° to 10° are shown in Table I. The value of the meridional loads in the dome, N_Φ' , the discontinuity load H and the moment M can be found from

$$N_\Phi' = \cot(\Phi_o - \omega)\; e^{-\lambda\omega}\left[\frac{2\lambda M}{a} \sin \lambda\omega - H\sqrt{2} \sin \Phi_o \sin\left(\lambda\omega - \frac{\pi}{4}\right)\right] \qquad (16)$$

Table II shows the value of N_Φ' for various values of ω .

The total stress is given by

$$f\Phi = \frac{N_\Phi{}^*}{t} \pm \frac{6M_\Phi}{t^2}$$

358

C

TABLE I

CALCULATION OF M_Φ

1	2	3	4	5	6	7	8
ω (degrees)	ω (radians)	$\lambda\omega$	$\lambda\omega + \frac{\pi}{4}$	$e^{-\lambda\omega}$	$\sin \lambda\omega$	$\sin\left(\lambda\omega + \frac{\pi}{4}\right)$	M_Φ
0	0	0	0.785	1.000	0	0.707	12.14
1	0.0174	0.523	1.308	0.592	0.502	0.965	0.15
2	0.0349	1.049	1.834	0.350	0.867	0.965	- 4.06
3	0.0524	1.574	2.360	0.207	1.000	0.705	- 4.21
4	0.0698	2.097	2.883	0.123	0.865	0.256	- 2.92
5	0.0873	2.623	3.408	0.072	0.496	-0.263	- 1.48
6	0.1047	3.146	3.931	0.043	-0.004	-0.708	- 0.51
7	0.1222	3.672	4.457	0.025	-0.506	-0.967	0
8	0.1396	4.194	4.980	0.015	-0.868	-0.963	0.17
9	0.1571	4.720	5.506	0.009	-1.000	-0.700	0.18
10	0.1745	4.243	6.028	0.005	-0.862	-0.253	0.12

$$M_\Phi = e^{-\lambda\omega}\left[17.162 \sin\left(\lambda\omega + \frac{\pi}{4}\right) - 32.480 \sin \lambda\omega\right]$$

(Intermediate Values Not Checked)

388

TABLE II

CALCULATION OF N_Φ'

1	2	3	4	5	6	7	8	9	10
ω (degrees)	ω (radians)	$\lambda\omega$	$\lambda\omega - \frac{\pi}{4}$	$\Phi_o - \omega$	$\cot(\Phi_o - w)$	$e^{-\lambda\omega}$	$\sin\lambda\omega$	$\sin\left(\lambda\omega - \frac{\pi}{4}\right)$	N_Φ'
0	0	0	-0.785	23°04'	2.348	1.000	0	-0.707	-64.16
1	0.0174	0.523	-0.262	22°04'	2.467	0.592	0.502	-0.259	-29.12
2	0.0349	1.049	0.264	21°04'	2.596	0.350	0.867	0.261	- 6.93
3	0.0524	1.574	0.789	20°04'	2.738	0.207	1.000	0.709	+ 3.96
4	0.0698	2.097	1.312	19°04'	2.893	0.123	0.865	0.966	7.00
5	0.0873	2.623	1.838	18°04'	3.066	0.072	0.496	0.964	5.99
6	0.1047	3.146	2.361	17°04'	3.257	0.043	-0.004	0.705	3.83
7	0.1222	3.672	2.887	16°04'	3.472	0.025	-0.506	0.252	1.75
8	0.1396	4.194	3.409	15°04'	3.715	0.015	-0.868	0.263	0.42
9	0.1571	4.720	3.935	14°04'	3.991	0.009	-1.000	-0.712	- 0.26
10	0.1745	5.243	4.458	13°04'	4.309	0.005	-0.862	-0.967	- 0.43

$$N_\Phi' = -\cot(\Phi_o - \omega)\, e^{-\lambda\omega}\left[20.430 \sin\lambda\omega - 38.653 \sin\left(\lambda\omega - \frac{\pi}{4}\right)\right]$$

(Intermediate Values Not Checked)

where $N_{\Phi}^* = N_{\Phi} + N_{\Phi}'$

The value of the stress for various values of ω is shown in Table III. The margin of safety is

$$M.\ S. = \frac{31900}{27930} - 1 = +0.14$$

The hatch ring is subjected to an overturning couple of

$$\begin{aligned} T &= M + He \\ &= 12.14 + 69.77(0.187) \\ &= 25.2 \text{ in.-lb/in.} \end{aligned}$$

This results in a bending stress of

$$\begin{aligned} f_b &= + \frac{Tr_o\, e}{I} \quad , \quad - \frac{Tr_o\, (d - e)}{I} \\ &= + \frac{Tr_o\, e}{\dfrac{d^3(c^2 + 4cb + b^2)}{36(c + b)}} \quad , \quad \frac{-Tr_o\, (d - e)}{\dfrac{d^3(c^2 + 4cb + b^2)}{36(c + b)}} \\ &= +9420 \text{ psi} \quad , \quad -13247 \text{ psi} \end{aligned}$$

In addition, it is subjected to a hoop stress of

$$\begin{aligned} f_h &= \frac{\left(H_o + H\right) r_o}{A} \\ &= \frac{\left(H_o + H\right) r_o}{d\, \dfrac{(b + c)}{2}} \\ &= -23{,}200 \text{ psi} \end{aligned}$$

Resulting in a maximum compressive stress of

$$f_c = -13247 - 23200 = -36447 \text{ psi}$$

for 7075-T6 aluminum alloy

$$F_{cy} = -61000 \text{ psi}$$

TABLE III

STRESSES IN DOME

ω	N_Φ'	N_Φ^*	N_Φ^*/t	M_Φ	$6M_\Phi/t^2$	f_Φ (outside)	f_Φ (inside)
0	-64.16	828	12180	12.14	15750	- 3570	27930
1	-29.12	863	12690	0.15	190	12500	12880
2	- 6.93	886	13030	- 4.06	- 5270	18300	7760
3	3.96	896	13180	- 4.21	- 5460	18640	7720
4	7.00	900	13240	- 2.92	- 3790	17030	9450
5	5.99	898	13210	- 1.48	- 1920	15130	11290
6	3.83	896	13180	- 0.51	- 660	13840	12520
7	1.75	894	13150	0	0	13150	13150
8	0.42	893	13130	0.17	220	12910	13350
9	- 0.26	892	13120	0.18	230	12890	13350
10	- 0.43	892	13120	0.12	160	12960	13280

$$N_\Phi^* = N_\Phi + N_\Phi' \quad , \quad N_\Phi = 892.5$$

Inside surface of dome: $f_\Phi = N_\Phi^*/t + 6M_\Phi/t^2$

Outside surface of dome: $f_\Phi = N_\Phi^*/t - 6M_\Phi/t^2$

C

Then,

$$M. S. = \frac{-61000}{-36447} - 1 = +0.67$$

4. <u>Shear Stress</u>

Shear stress in laminate at the inside edge of ring:

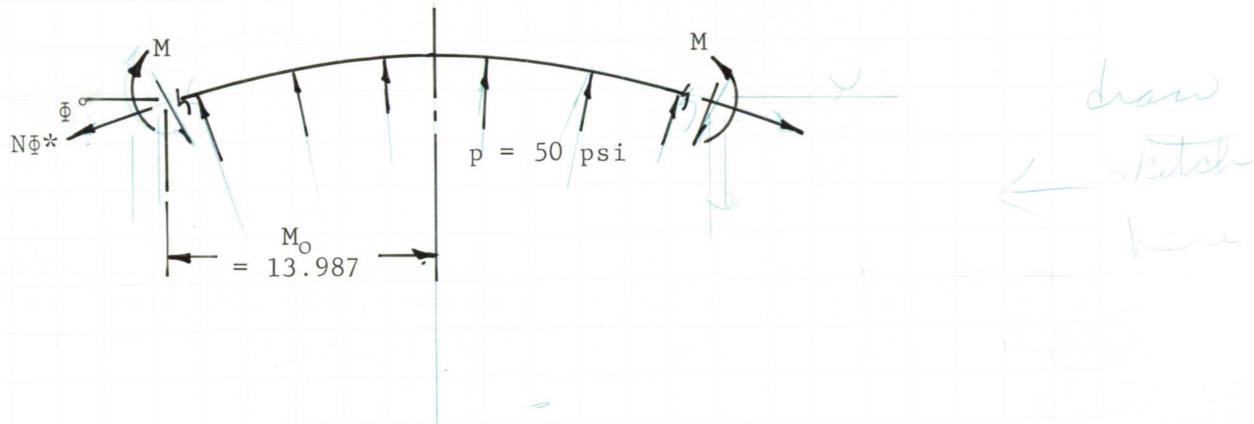

$$\Phi_o = 23°04'$$

$$\Sigma FV = 0$$

$$pr_o = N_\Phi * \sin \Phi_o \ (2) + V \cos \Phi_o \ (2)$$

$$V = \frac{pr_o - ZN_\Phi * \sin \Phi_o}{2 \cos \Phi_o}$$

$$= \frac{50(13.987) - 2(828)(0.39180)}{2(0.92005)}$$

$$= 27.46 \text{ lb/in. ultimate}$$

$$f_s = \frac{VQ}{I} = \frac{3}{2} \cdot \frac{V}{A} = \frac{3}{2} \cdot \frac{27.46}{1(0.068)}$$

$$= 608 \text{ psi}$$

APPENDIX D

RING (TOP END) ANALYSIS

The configuration of the ring is shown in Drawing Nr. 291.

1. Rotational Deflection (Slope)

For the purpose of analysis, the inner portion of the ring, from the diameter of 30.00 inches to 33.40 inches, can be considered as a flat plate with its outer edge (33.60 diameter) fixed, as shown below.

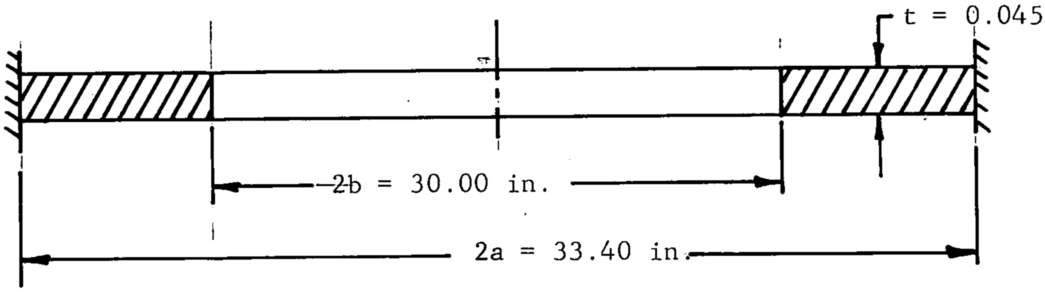

This plate is subjected to a load W applied at its inner edge equal to the total load on the hatch, and a load distributed over its entire surface W equal to the internal pressure of the airlock. The scope of the plate at any point θ is a function of the load W , the load w , and the fixed end moment M_a . At the outer edge (fixed edge) the slope equals zero ($\theta_0 = 0$) . The slopes at the outer edge due to the three loadings are[4]:

$$\theta_{0_1} = \frac{12a}{Et^3} \left[M_a \frac{(1-\mu) + (b/a)^2 (1+\mu)}{1 - (b/a)^2} \right] \tag{1}$$

$$\theta_{0_2} = \frac{3 W_a (1-\mu^2)}{\pi E t^3} \left[\frac{1}{1+\mu} + \frac{2}{1-\mu} \cdot \frac{(b/a)^2}{1-(b/a)^2} \ln a/b \right] \tag{2}$$

$$\theta_{o_3} = \frac{w\,a^3}{2\,Et^3}\left[3\,(1-\mu) + (3+9\mu)\left(\frac{b}{a}\right)^2 - 12\,(1+\mu)\,\frac{(b/a)^4}{1-(b/a)^2}\,\ln\frac{a}{b}\right] \qquad (3)$$

where

θ_{o_1} = slope at outer edge due to fixed end moment, M_a

θ_{o_2} = slope at outer edge due to load W

θ_{o_3} = slope at outer edge due to load w

a = outer radius = 16.700 in.

b = inner radius = 15.000 in.

M_a = fixed end moment

μ = Poisson's ratio = 0.33

E = modulus of elasticity of plate = 10.3×10^6 psi

t = thickness = 0.45 in.

w = pressure load on plate = -50 psi

W = total load on hatch = $w \pi b^2$ = 35,325 lb

Substituting these values into equation (1) through (3)

θ_{o_1} = 0.0019260 M_a radians (see Note 1)

θ_{o_2} = 1.1167052 radians (see Note 1)

θ_{o_3} = 1.1319182 radians (see Note 1)

Equating $\sum_1^n \theta_{o_n}$ to zero, and solving for M_a yields M_a = 648.30 in.-lb/in.

The slope of the inner edge of the plate (ring) due to each of the three loadings can be found from

$$\theta_{i_1} = \frac{12\,a}{E\,t^3}\left[2\,M_a\,\frac{b/a}{1-(b/a)^2}\right] \qquad (4)$$

Note 1: The large number of significant figures carried throughout the above analysis is necessary because number very close in magnitude are subtracted from each other.

2

$$\theta_{i_2} = \frac{3\ W\ a(1-\mu^2)}{\pi\ E\ t^3} \left[\frac{b/a}{1+\mu} + \frac{2}{1-\mu}\ \frac{b/a}{1-(b/a)^2}\ \ln\frac{a}{b} \right] \tag{5}$$

$$\theta_{i_3} = \frac{w\ a^3}{2\ E\ t^3} \left[3\ (3+\mu)\left(\frac{b}{a}\right) - 3\ (1-\mu)\left(\frac{b}{a}\right)^3 - 12\ (1+\mu)\ \frac{(b/a)^3}{1-(b/a)^2}\ \ln\frac{a}{b} \right] \tag{6}$$

Substituting the appropriate values into equations (4) through (6),

θ_{i_1} = 1.2868503 radians (see Note 1)

θ_{i_2} = 1.1567544 radians (see Note 1)

θ_{i_3} = 0.1365034 radians (see Note 1)

Then the slope at the inner edge is

$$\theta_i = \sum_1^3 \theta_{i_n} = -0.00641 \text{ radians}$$

To this slope, the slope of the "fixed edge" caused by the rotation of the remainder of the ring must be added. The effective cross-section for this portion of the analysis is estimated to be as shown below. The solid lines indicate the effective area, the phantom lines indicate the actual ring configuration. As can be seen, a portion of the retainer (Drawing Nr. 292) is considered to be effective. The total moment on this section about point A is

$$M_a = -M_a - 2.23\ W_1 + (2.23)^2\ w$$

Note 1: The large number of significant figures carried throughout the above analysis is necessary because number very close in magnitude are subtracted from each other.

3

388-077

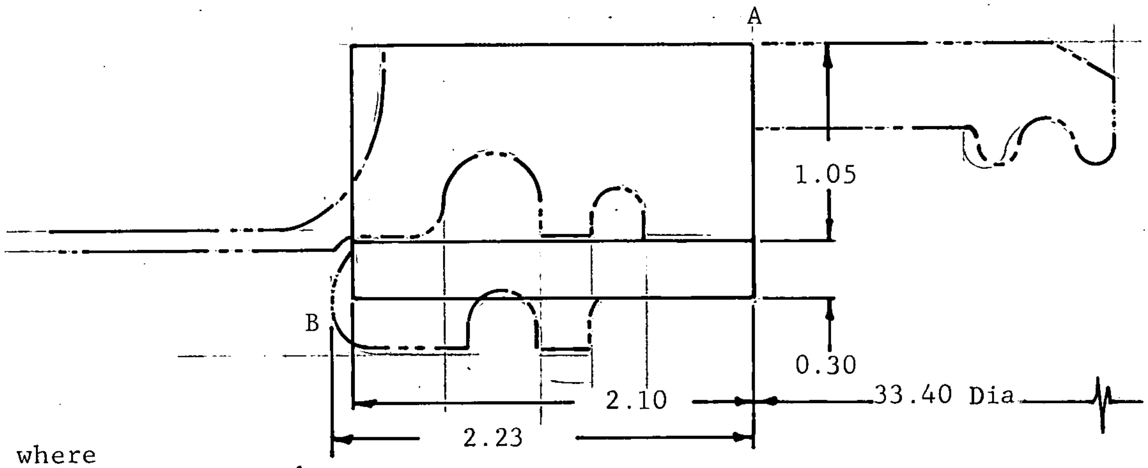

where

W_1 = axial component of load in fabric (at Point B)

= p (37.86)/4 = 473.25 lb/in.

p = 50 psi

w - pressure load = 50 psi

Then

$$M_A = -648 - 1055 + 249 = -1454 \text{ in.-lb/in.}$$

From Roark[8] the slope of the ring is

$$\theta_R = \frac{M_A r^2}{EI} \tag{7}$$

where

r = average radius of effective section = 17.75 in.

$$\theta_R = \frac{-1454\ (17.75)^2}{10.3 \times 10^6\ \frac{2.10(1.35)^3}{12}} = -0.10330 \text{ radians}$$

The total slope of the upper ring at the dome seal is then

$$\theta = \theta_i + \theta_R = -0.00641 - 0.10330 = -0.10971 \text{ radians} = 6.3°$$

4

2. Stress

a. Considering the inner portion of the ring as a flat plate, as before, the maximum stress will occur at its outer edge in the radial direction. The stress is given by Roark[9] for the two loading conditions as

$$f_1 = \frac{3w}{4t^2}\left[a^2 - 2b^2 + \frac{b^4(m-1) - 4b^4(m+1)\ \ln a/b + a^2b^2(m+1)}{a^2(m-1) + b^2(m+1)}\right] \quad (8)$$

$$f_2 = \frac{3W}{2\pi t^2}\left[1 - \frac{2\ m\ b^2 - 2b^2(m+1)\ \ln \frac{a}{b}}{a^2(m-1) + b^2(m+1)}\right] \quad (9)$$

where

f_1 = stress due to uniform load w , psi

f_2 = stress due to load W , psi

m = $1/\mu$ = 3.0

All other parameters as previously defined on page 79.

f_1 = 2,030 psi

f_2 = 17,185 psi

Then

$$f = f_1 + f_2 = -19,215 \text{ psi}$$

For 7075-T6 aluminum alloy[10]

$$F_{cy} = -61,000 \text{ psi}$$

The margin of safety is

$$\text{M.S.} = \frac{-61,000}{-19,215} - 1 = +2.17$$

For the remainder of the ring (effective section shown on page 80).

$$f = \pm \frac{M_A\ r}{I/c} \qquad (10)$$

where

f = stress in ring

c = $(1.05 + 0.30)/2 = 0.675$

f = $\mp 18{,}040$ psi

MS = $\frac{61{,}000}{18{,}040} - 1 = +2.38$

b. <u>Outer Segment</u>

The outer segment of the ring can be considered to be a flat plate with its inner edge fixed. During the folding operation there is a total load of 400 pounds on this segment. Then, from Roark,* the maximum stress occurs at the inner edge and is given by

$$f = \frac{3\,w}{4\ t^2}\left[\frac{4a^4(m+1)\ \ln\frac{a}{b} - a^4(m+3) + b^4(m-1) + 4a^2b^2}{a^2(m+1) + b^3(m-1)}\right] \qquad (11)$$

$$y = \frac{3w(m^3-1)}{16m^2\ Et^3}\left\{a^6(7m+3) + b^6(m-1) - a^4b^2(m+7) - a^2b^4(7m-5) - 4a^2b^2\left[a^2(5m-1) + b^2(m+1)\right]\ln\frac{a}{b} 16a^4b^2(m+1)\left(\ln\frac{a}{b}\right)^2\right\} \Big/ \left[a^2(m+1) + b^2(m-1)\right] \qquad (12)$$

where

w = uniform load on surface = $\frac{400}{\pi(a^2-b^2)} = 1.1654$ psi

t = thickness = 0.100 in.

a = outside radius = 21.25 in.

b = inside radius = 18.50 in.

m = $1/\mu = 3.0$

μ = Poisson's ratio = 0.33

E = modulus of elasticity = 10×10^6 psi

6

Then

$$f = 2,840 \text{ psi}$$
$$y = -0.013 \text{ in.}$$

c. Bolt Holes

It is necessary to check for stripping of the threads in the bolt holes. The length of thread required is[11]

$$Q = J\,L_e \tag{13}$$

$$J = \frac{A_s \times \text{tensile strength of external thread material}}{A_n \times \text{tensile strength of internal thread material}} \tag{14}$$

$$A_s = 3.1415\, nL_e\, K_n\max \left[\frac{1}{2n} + 0.57735\left(E_s \min - K_n \max\right)\right] \tag{15}$$

$$A_n = 3.1416\, nL_e\, D_s\min \left[\frac{1}{2n} + 0.57735\left(D_s \min - E_n \max\right)\right] \tag{16}$$

$$L_e = \frac{2\,A_t}{3.1416\, nK_n \max\left[\frac{1}{2n} + 0.57735\left(E_s \min - K_n \max\right)\right]} \tag{17}$$

$$A_t = 3.1416\left(\frac{E_s \min}{2} - \frac{0.16238}{n}\right)^2 \tag{18}$$

where

L_e = length of engagement when $J \le 1.0$

J = see equation (14)

Q = length of engagement when $J > 1.0$

A_s = A_n = shear areas of external threads

n = number of threads/inch

$K_n max$ = maximum minor diameter of internal thread

$E_s min$ = minimum pitch diameter of external thread

A_t = tensile stress area of screw thread

$D_s min$ = minimum major diameter of external thread

$E_n max$ = maximum pitch diameter of internal thread

For the threads specified, 5/16-18 unc Class 2B internal and 5/16-18 unc Class 3A external,[12]

$$n = 18$$
$$K_n max = 0.265$$
$$E_s min = 0.2734$$
$$D_s min = 0.3038$$
$$E_n max = 0.2817$$
$$A_t = 0.051214 \text{ in.}^2$$
$$L_e = 0.209493 \text{ in.}$$
$$A_s = 0.102424 \text{ in.}^2$$
$$A_n = 0.145890 \text{ in.}^2$$

The tensile strength of the aluminum is 61,000 psi, and that of the bolts is 5660[13]/A_t = 110,500 psi. Then

$$J = \frac{0.102424\ (110,500)}{0.145890\ (61,000)} = 1.272$$

and

$$Q = 1.272\ (0.209493) = 0.266 \text{ in.}$$

The actual thread engagement is 0.449 (with bolt length at minimum tolerance). The ratio of actual to required thread engagement is greater than 1.0. Therefore, the number of bolts required can be based upon bolt strength as was done in the analysis of "Retainer-Structural Fabric-Airlock."

9

APPENDIX E

BASEPLATE ANALYSIS

STRESS AND DEFLECTION

The configuration of the baseplate is shown in drawing NR 284. For analysis, this is assumed as a circular flat plate fixed at its outside diameter (fixed at the bolt circle diameter of 51.750 in.). It is loaded at its inner diameter (33.40 in.). Then, from Roark[14], the maximum stress occurs at the outer edge in the radial direction and is given by

$$f = \frac{3\omega}{2\pi t^2}\left[1 - \frac{2mb^2 - 2b^2(m+1)\ln\frac{a}{b}}{a^2(m-1) + b^2(m+1)}\right] \qquad (1)$$

and the maximum deflection is

$$y = -\frac{3\omega(m^2-1)}{4\pi m^2 E t^3}\left[\frac{2mb^2(a^2-b^2) - 8ma^2b^2\ln\frac{a}{b} + 4a^2b^2(m+1)\left(\ln\frac{a}{b}\right)^2}{a^2(m-1) + b^2(m+1)} + a^2 - b^2\right] \qquad (2)$$

where

f = Maximum stress, psi

ω = Total load = $p\pi b^2$ = $50(3.14)(16.7)^2$ = 43785 lb.

m = 1/Poisson's ratio = 1/0.33 = 3.0

b = Inner radius = 16.70 in.

a = Outer radius = 25.875 in.

t = Thickness = 1.0 in.

E = Modulus of elasticity = 9.9×10^6 psi

then

$$f = 14970 \text{ psi}$$

and

$$\bar{y} = 0.086 \text{ in.}$$

The allowable stress for 6D61-T651 aluminum alloy is

$$F_{ty} = 35000 \text{ psi}$$

Then the margin of safety is

$$\text{M. S.} = \frac{35000}{14970} - 1 = +1.34$$

BOLT HOLES

The analysis for the bolt holes is identical to that of the "Ring-Top End Airlock" analysis (pp. 8 and 9 of that analysis) up to the calculation of J .

$$J = \frac{0.102424(110500)}{0.145890(35000)} = 2.217$$

$$Q = J\,Le = 2.217(0.209493) = 0.464$$

The actual thread engagement is 0.449 in. The ratio of actual to required thread engagement is less than 1.0 (0.449/0.464 = 0.968). Therefore, the number of bolts required must be based upon thread strength rather than bolt strength. Refering to page 2 of the analysis of the "Retainer-Structural Fabric-Airlock," the allowable tensile load per bolt is reduced to 5660(0.968) = 5418 lb. Then, the number of bolts required is

$$N_B = \frac{R_B C_B}{5418} = \frac{2450(107.262)}{5418} = 49$$

The margin of safety becomes

$$\text{M. S.} = \frac{64}{49} - 1 = +0.31$$

388

APPENDIX F

AIRLOCK BASEPLATE COVER ANALYSIS

BASEPLATE COVER ANALYSIS

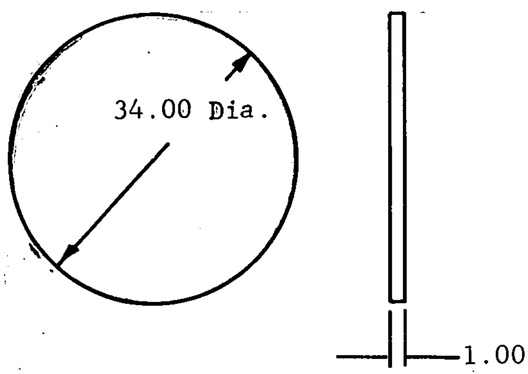

Critical Loading Conditions:

1. 50 psi burst
2. 30 psi test
3. 10 psi operating

Material: 2024 T42 aluminum alloy

$Ftu = 62,000$ psi
$Fty = 40,000$ psi

Check St max

$$St_{max} = \frac{3W}{8\pi m t^2}(3M + 1)$$

$$m = \frac{1}{\upsilon} = \frac{1}{0.33} = 3$$

$$\text{Area} = 17^2 \times 3.14 = 908 \text{ in.}^2$$

For 50 psi,

$$St_{max} = \frac{3 \times 908 \times 50(9 + 1)}{8 \times 3.14 \times 1^2} = \frac{1.365 \times 10^6}{75.5} = 18,100 \text{ psi}$$

For 30 psi,

$$St_{max} = \frac{3 \times 908 \times 30(10)}{75.5} = 10,800 \text{ psi}$$

For 10 psi,

$$St_{max} = \frac{3 \times 908 \times 30(10)}{75.5} = 10,800 \text{ psi}$$

F1

Check y_{max} at Center

$$y_{max} = \frac{-3W(m - 1)(5m + 1)a^2}{16\pi E m^2 t^3}$$

For 50 psi,

$$y_{max} = \frac{-3 \times 908 \times 50(3 - 1)[5(3) + 1]\ 17^2}{16 \times 3.14 \times 10 \times 10^6 \times 9 \times 1^3}$$

$$= \frac{136,500(2)(16)290}{4550 \times 10^6} = \frac{1265}{4550} = 0.28 \text{ in.}$$

For 30 psi,

$$y_{max} = \frac{3 \times 908 \times 30(2)(16)(290)}{4550 \times 10^6}$$

$$= \frac{760 \times 10^6}{4550 \times 10^6} = 0.168 \text{ in.}$$

For 10 psi,

$$y_{max} = \frac{3 \times 908 \times 10(\eta)(16)(290)}{4550 \times 10^6}$$

$$= \frac{253 \times 10^6}{4550 \times 10^6} = 0.056 \text{ in.}$$

Check Attachment Bolts Load Capability

Ultimate tensile capacity of shcs = 10,100 lb/each

32 X 10,000 = 323,200 lb total capacity

Total load = 290 X 50 = 14,500 lb

M. S. = 323,200/14,500 = 22/1

F

388

Allowable Out-of-Roundness of Cable Windup Ring

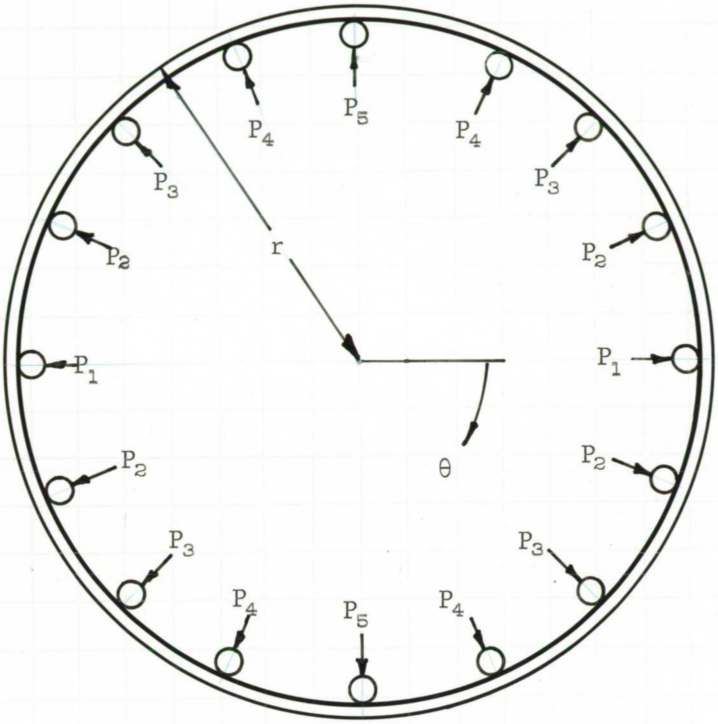

Run picture here

Assume a loading distribution as shown above with

$$P_1 = 600 \text{ lb}$$
$$P_2 = 525 \text{ lb}$$
$$P_3 = 150 \text{ lb}$$
$$P_4 = 75 \text{ lb}$$
$$P_5 = 0 \text{ lb}$$

Then the deflection of the ring will be

$$u = \frac{P_1 r^3}{EI}\,[0.25 \sin\theta + (0.3927 - 0.25\theta)\cos\theta - 0.3183] +$$

$$\frac{P_2 r^3}{EI}\,\{0.25 \sin(22.5° - \theta) + [0.3927 - 0.25(22.5° - \theta)]\cos(22.5° - \theta) -$$

F3

$$- 0.3183\} + \frac{P_3 r^3}{EI} \{0.25 \sin(45° - \theta) + [0.3927 - 0.25(45° - \theta)] \cdot \cos(45° - \theta) - 0.3183\} + \frac{P_4 r^3}{EI} \{0.25 \sin(67.5° - \theta) + [0.3927 - 0.25(67.5° - \theta)] \cos(67.5° - \theta - 0.3183\} + \frac{P_4 r^3}{EI} \{0.25 \sin(112.5° - \theta) + [0.3927 - 0.25(112.5° - \theta)] \cos(112.5° - \theta) - 0.3183\} + \frac{P_3 r^3}{EI} \{0.25 \sin(135° - \theta) + [0.3927 - 0.25(135° - \theta)] \cos(135° - \theta) - 0.3183\} + \frac{P_2 r^3}{EI} \{0.25 \sin(157.5° - \theta) + [0.3927 - 0.25(157.5° - \theta)] \cdot \cos(157.5° - \theta) - 0.3183\}$$

where

u = radial deflection at any point, in.
r = radius of ring = 50 in.
E = modulus of ring = 10×10^6 psi
I = moment of inertia of ring cross-section = 0.11 in^4

At $\theta = 0$

$$u = 6.82(0.3927 - 0.3183) + 4.97[0.096 + (0.3927 - 0.098)\ 0.924 - 0.3183] + 1.70[0.177 + (0.3927 - 0.196)\ 0.707 - 0.3183] + 0.85[0.231 + (0.3927 - 0.294)\ 0.383 - 0.3183] + 0.85[0.231 - (0.3927 - 0.442)\ 0.383 - 0.3183] + 1.70[0.177 - (0.3927 - 0.589)\ 0.707 - 0.3183] + 5.97\ [0.096 - (0.3927 - 0.688)\ 0.924 - 0.3183]$$

$u = 1.00$ in.

This shows that the roundness tolerance of the ring, to remain within allowable loads on the bearing supports, is not critical.

APPENDIX G

OVERLAP LENGTH DETERMINATION FABRIC JOINT AIRLOCK

The following sketch is a schematic of the airlock fabric specimen-strand loads.

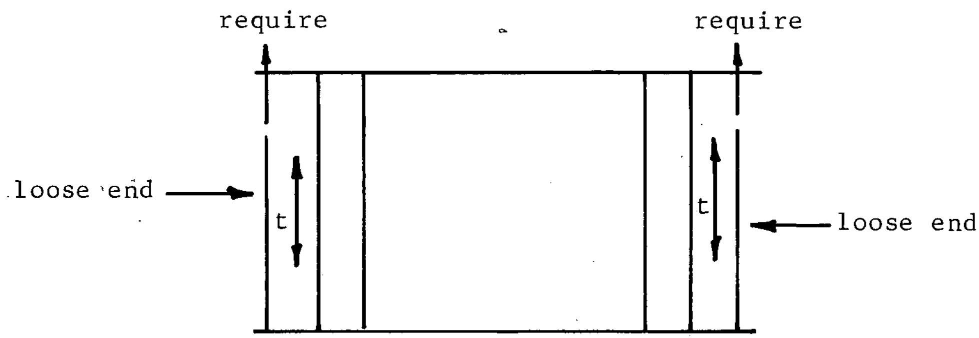

At failure there should be a net tension in each strand. Therefore, the loose end should be fixed. Since there are only two end rods and the fabric specimens must be slipped from the dowels to the rods, it will be practicle to bond the loose ends to adjacent strands. However, this will change the distribution of the load end, the two end strands, somewhat reducing the net tension in each strand over partial lengths of the strands.

Assuming a lap shear type joint, the length of the bondline can be calculated. Assume the load in the joint will be 100 pounds (T), the adhesive shear is 3,000 psi, and the width of the joint is the fiber diameter 0.020 inch, the length of the joint is L .

T = 100 lb (load)

t_A = ultimate tensile shear of the adhesive = 3,000 psi

w = 0.020 in. fiber diameter — joint width

L = length of overlap — to be determined.

$$T = t_A wL \quad , \quad L = \frac{T}{t_A w}$$

$$L = \frac{100}{3{,}000\ (0.020)} = \frac{100}{60}$$

$$L = 1.67 \text{ in.}$$

Actual strand failure should occur at 80 pounds. T with overlap of 2 inches is:

$$T = 3{,}000\ (0.020)\ (2) = 120 \text{ pounds}$$

Margin of Safety

$$M.S. = \frac{120}{80} - 1 = 1.5 - 1 = +0.50$$

If a stronger adhesive shear strength and wider effective bond width is obtained, the margin of safety is higher. With a 3.0 inch overlap

$$T = 3{,}000\ (0.020)\ (3) = 180 \text{ pounds}$$

$$M.S. = \frac{180}{80} - 1 = 2.25 - 1 = +1.25$$

APPENDIX H

STRUCTURAL FABRIC RETAINER ANALYSIS

NUMBER OF BOLTS

The configuration of the retainer is shown in Drawing Nr 292. It is first necessary to determine the number of bolts required to hold the retainer in place. Considering the cross-section of the retainer to be a beam as shown below

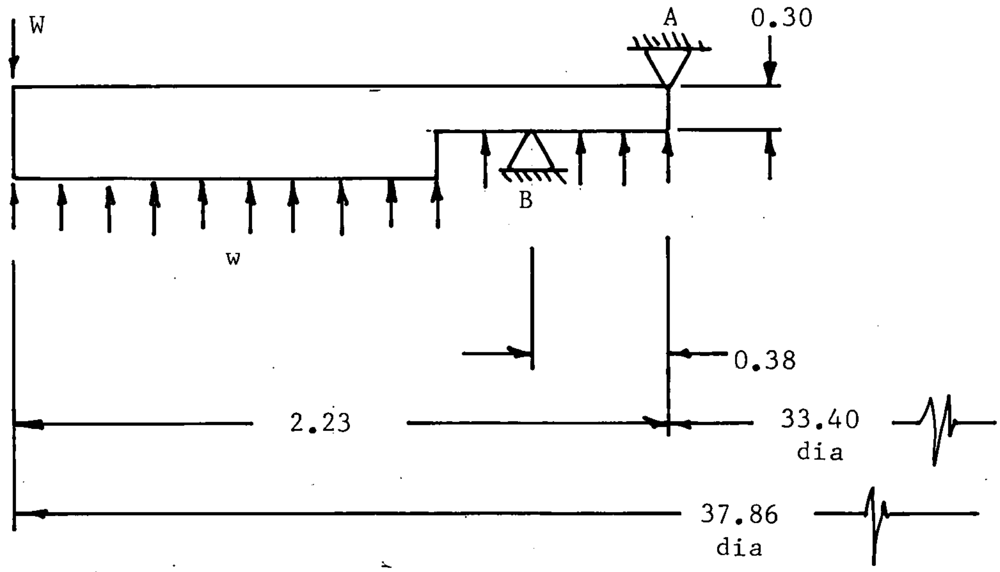

The reaction at Point B (which represents the bolts) can be determined by taking moments about Point A. Then, for equilibrium

$$EM_A = 0 = -2.23\ W + \frac{(2.23)^2\ W}{2} + 0.38\ R_B$$

where

W = axial component of load in fabric = $\frac{p(37.86)}{7}$ lb/in.

w = 50 psi

p = 50 psi

Then,

$$R_B = \left[2.23 \frac{50\ (37.86)}{4} - \frac{(2.23)^2\ (50)}{2} \right] \Bigg/ 0.38 = 2{,}450 \text{ lb/in.}$$

The circumference of the bolt circle diameter is

$$C_B = \left[33.40 + 2(0.38) \right] \pi = 107.262 \text{ in.}$$

The allowable tensile load of the bolt (MS 20074-05) is 5660 lb. Then the required number of bolts is

$$N_B = \frac{R_B\ C_B}{5660} = 46 \text{ bolts}$$

The margin of safety is

$$\text{M.S.} = \frac{64}{46} - 1 = +0.39$$

<u>BENDING STRESS</u>

The bending moment is a maximum at Point B and is equal to

$$M_B = -(2.23-0.38)\ W + \frac{(2.23-0.38)^2\ w}{2}$$

$$= -(2.23-0.38) \frac{50\ (37.86)}{4} + \frac{(2.23-0.38)^2\ (50)}{2}$$

$$= -790 \text{ in./lb/in.}$$

Then the stress is

$$f_b = \pm \frac{M\ c}{I} = \pm \frac{-790 \left(\frac{0.30}{2}\right)}{\frac{1\ (0.30)^3}{12}}$$

$$= \mp 52{,}670 \text{ psi}$$

H

The allowable strength (7075-T6) is[10]

$$F_{ty} = F_{cy} = 64{,}000 \text{ psi}$$

Then the margin of safety is

$$M.S. = \frac{64{,}000}{52{,}670} - 1 = +0.22$$

APPENDIX I

WEIGHT ANALYSIS

NR 303 — ARM CABLE ATTACHMENT — AIRLOCK

-7 arm. 2024-T4 aluminum ($\rho = 0.1$ lb/in.^{3})

$$\text{Volume} = 4.53 \text{ in.}^3$$

$$\text{Weight} = 4.53 \times 0.1 = 0.45 \text{ lb}$$

4 to 7 arms required

$$4 \times 0.45 = 1.80 \text{ lb}$$

NR 302 — MISCELLANEOUS SEALS — AIRLOCK

Material: butyl ($\rho = 0.045$ lb/in.^{3})

$$\text{Diameter} = 0.25 \text{ in.}$$

$$\text{Area} = \pi \cdot \frac{0.25^2}{4} = 0.049 \text{ in.}^2$$

-7 — 1 required

$$\text{Weight} = 0.045 \times 0.049 \times 50.32\,\pi = 0.348 \text{ lb}$$

-9 — 3 required

$$\text{Weight} = 3 \times 0.0022 \times 34.85\,\pi = 0.722 \text{ lb}$$

-11 — 1 required

$$\text{Weight} = 0.0022 \times 30.50\,\pi = 0.211 \text{ lb}$$

-13 — 1 required

$$\text{Weight} = 0.0022 \times 30.50\,\pi = 0.211 \text{ lb}$$

Total Seals Weight = 1.492 lb

NR 301 — SPACER-ROLLER — AIRLOCK

Material: 6061 aluminum ($\rho = 0.10$ lb/in.^{3})

$$\text{Volume} = 1.00 \cdot \frac{\pi}{4} (0.75^2 - 0.315^2)$$

$$= 0.364 \text{ in.}^3$$

16 required:

$$\text{Weight} = 16 \times 0.364 \times 0.1 = 0.581 \text{ lb}$$

NR 300 — TENSIONER, CABLE — AIRLOCK

Material: S. Steel 17-7 ph ($\rho = 0.276$ lb/in.^{3})

$$\text{Volume} = 0.866(0.870^2) \times 0.31 + \frac{\pi}{4} (0.375^2)\ 2.0$$

$$= 0.203 + 0.221 = 0.424 \text{ in.}^3$$

4 required:

$$\text{Weight} = 4 \times 0.276 \times 0.424 = 0.468 \text{ lb}$$

NR 299 — BLEED VALVE INSTALLED

-9 and -11	= -7	Assorted Handles (2 required)	2.52 lb
	-17	Stem	0.29
	-19	Valve Body (Titanium)	0.34
	-21	Nuts (2 required)	0.02
	-13	Doubler	0.10
		TOTAL	3.27 lb

NR 298 — IDLER PULLEY ASSEMBLY

-7 Pulley (4 required) $\rho = 0.10$

$$\frac{\pi}{4} (1.599)^2 \times 0.312 \times 4 \times 0.10 = 0.25$$

Brackets (4 required):

Weight = 0.72 lb

Total Weight = 0.97 lb

I-2

NR 297 — HATCH LATCH ASSEMBLY

-7 Bracket: Aluminum $\rho = 0.10$

Weight $= 0.094 \times 0.69\ (1.1 + 1.1 + 1.63) \times 0.1 = 0.025$ lb

4 required for a total of 0.100 lb

-11 pin: 8 required S. Steel $\rho = 0.286$

Weight $= 8 \times 0.027 \times 1.13 \times 0.286 = 0.07$ lb

-9 plate: 4 required

Weight $= 4 \times 0.320 \times 1.06 \times 0.125 \times 0.286 = 0.049$ lb

Total Weight = 0.219 lb

NR 296 — HATCH DOME

1 required: 181 E Glass-Epoxy $\rho = 0.067\ \text{lb/in}^3$

$$\text{Area} = 2\pi\ (21.4)(6.5) + 6\pi$$

$$= 873 + 57 = 930\ \text{in}^2$$

$$\text{Weight} = 0.060\ (930)(0.067) = 3.74\ \text{lb}$$

NR 295 — HATCH RING

1 required: Aluminum $\rho = 0.10\ \text{lb/in}^3$

$$\text{Weight} = 30.75\pi \times 0.45 \left(0.5 + \frac{0.45}{2}\right) \times 0.10 = 3.15\ \text{lb}$$

NR 294 — HATCH ASSEMBLY

NR 299 Bleed Valve	3.27 lb
NR 296 Hatch Dome	3.74
NR 295 Hatch Ring	3.15
Adhesive	0.25
TOTAL NR 294	10.41 lb

NR 292 — RETAINER STRUCTURAL FABRIC

Material: Aluminum 2024 $\rho = 0.10 \text{ lb/in}^3$.

Weight = $[2.11(0.90) -).75(0.2)] \times 35.29\pi \times 0.10 = 9.95$ lb

NOTE: 1 each required at hatch ring and base.

NR 291 — RING ASSEMBLY HATCH END

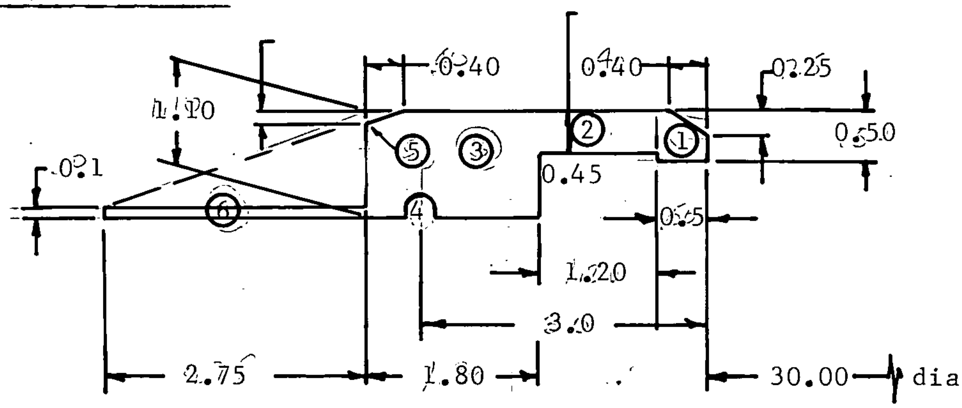

Item	Size	A	μ	Aμ
1	0.5×0.5	0.25	0.25	0.063
2	1.20×0.45	0.54	1.10	0.594
3	1.80×1.10	1.98	2.60	5.15
4	$\pi(0.2)^2$	-0.125	3.00	-0.37
5	$\frac{0.1}{2} \times 0.40$	-0.02	3.30	-0.065
6	$\frac{0.4}{0.2} \times 0.25$	-0.05	0.15	-0.075
Σ		2.85		6.642

$$\bar{y} = \frac{6.567}{2.82} = 2.33$$

$$\overline{\text{dia}} = 30.00 + 2.33 = 32.33$$

$$\text{Weight} = \text{Aring (Davg)} (\rho) + 4(7)$$

$$\text{Weight} = 2.85\ (32.33)\pi(0.10) + 4\left(\frac{2.6}{2} \times 0.75 \times 1.9\right)(0.10)$$

I-4

Weight = 28.94 + 0.74 = 29.69 lb (less holes 0.28)

NR 303 = 1.80

TOTAL 31.20

NR 287 — RETRACTION RING ASSEMBLY

-7 Ring: Aluminum $\rho = 0.10$

$$\text{Area} = 0.80\left(\frac{1.45 + 0.90}{2}\right) = 0.935 \text{ in}^2$$

$$D_{avg} = 48.05 \text{ in.}$$

$$\text{Weight} = 0.935\ (48.05)\pi(0.1) = 14.1 \text{ lb}$$

-13 Chain: 88 in. length — 0.085 lb/ft

Weight = 0.62 lb

Total Weight = 14.72 lb

NR 285 — COVER BASEPLATE

1 required: Aluminum

$$\text{Weight} = \left(\frac{\pi}{4}\ 36^2\right) \times 0.1 = 102 \text{ lb}$$

NR 284 — BASEPLATE

Material: Aluminum $\rho = 0.1 \text{ lb/in}^3$

$$\text{Weight} = 1867.91 \text{ in}^3 \times 0.1$$

$$\text{Weight} = 186.7 \text{ lb}$$

APPENDIX J

DESIGN DRAWINGS

For reference purposes, the list below summarizes the design drawings for the expandable airlock and their respective NASA/LRC numbers.

NASA/LRC NO.	DRAWING NO.	SIZE	TITLE
151,881	NR-282	X	Test Instl — Airlock
151,882	NR-283	X	Airlock Assy
151,883	NR-284	E	Base Plate — Airlock
151,884	NR-285	E	Cover — Base Plate — Airlock
151,885	NR-286	E	Liner Instl — Airlock
151,886	NR-287	E	Retraction Ring Assy — Airlock
151,887	NR-288	E	Shield — Retraction Mech. — Airlock
151,888	NR-289	D	Lanyard — Latch — Airlock
151,889	NR-290	X	Drive Unit Instl — Airlock
151,890	NR-291	E	Ring Assy — Top End — Airlock
151,891	NR-292	E	Retainer — Structural Fabric — Airlock
151,892	NR-293	E	Electrical Connector Instl — Airlock
151,893	NR-294	E	Hatch Assy — Airlock
151,894	NR-295	E	Hatch Ring — Airlock
151,895	NR-296	E	Hatch Dome — Airlock
151,896	NR-297	R	Hatch Latch Assy — Airlock
151,897	NR-298	R	Idler Pulley Assy — Airlock
151,898	NR-299	E	Bleed Valve Instl — Airlock
151,899	NR-300	A	Tensioner — Cable — Airlock
152,000	NR-301	A	Spacer — Roller — Airlock
152,001	NR-302	D	Seals — Airlock
152,002	NR-303	D	Arm — Cable Attach — Airlock
152,003	NR-309	E	Assy — Table — Airlock 15
152,004	NR-310	E	Handling Sling — Airlock
152,005	NR-313	D	Proof Pressure Test Schematic — Airlock
152,006	NR-316	A	Washer — Retraction Shield — Airlock
152,007	NR-317	A	Clip — Hatch Lanyard — Airlock
152,008	NR-351	A	Schematic of Fabric Specimen — Airlock
152,009	NR-352	E*	Fabric End Ring — Airlock

* Approximately.

APPENDIX K

MAINTENANCE

The nature of the airlock construction materials and configuration, as well as the exposed location of the retracting mechanism, require that care be taken in their assembly and installation. In particular, the following instructions must be observed:

1. Both ends of a linear element of the liner must be attached to the same relative position on the top and bottom end rings; that is, the liner must be assembled as a cylinder without any twisting of its linear elements.
2. The 64 bolts holding the structural fabric retainer (NR-292) to the airlock base plate (NR-284) must be torqued during assembly to 150 inch-pounds.
3. Before retracting the airlock the location and condition of retracting cables should be checked to ensure that the cables are properly in the grooves of retraction ring.
4. Before pressurizing the airlock, the liner must be positioned to prevent overstressing of sections of the liner. In other words, after deployment, the liner should be positioned to follow the convoluted contours of the lock. If this is not done, the friction between liner and structural fabric will prevent the free movement of the liner, resulting in overextension and stressing in one area, and looseness in another.

REFERENCES

1. Al Frazer, Airlock Structural Fabric, Final Report, Contract NAS 1-5752, Purchase Order 47037, Astro Research Corporation, Santa Barbara, California, 1968.
2. H. Schuerch and A. Kyser, Structural and Folding Analysis of the Airlock, Report ARC R-169, Astro Research Corporation, Santa Barbara, California, 16 October 1964.
3. Technical Data Sheets on Properties of Filament Wound S-Glass/Epoxy Composites, US Polymeric Chemicals Inc.
4. R. J. Roark, Formulas for Stress and Strain, third edition, McGraw-Hill Book Company Inc., 1954, pp. 226-227.
5. S. Timoshenko, Theory of Plates and Shells, second edition, McGraw-Hill Book Company Inc., 1959, pp. 555-557.
6. Ibid., pp. 550-551.
7. Roark, Op. Cit., pp. 226-227.
8. Ibid., pp. 230-231.
9. Ibid., p. 199.
10. Mil-Hdbk-5, August 1962.
11. E. Oberg and F. D. Jones, Machinery's Handbook, sixteenth edition, Industrial Press, pp. 1050-1051.
12. Ibid., p. 1126.
13. Specification MS 20074.
14. Roark, Op. Cit.